Comparative analyses of hydrological responses of two adjacent watersheds to climate variability and change using the SWAT model

Sangchul Lee[1,2], In-Young Yeo[3,4], Ali M. Sadeghi[2], Gregory W. McCarty[2], Wells D. Hively[5], Megan W. Lang[4,6], Amir Sharifi[7]

[1] Department of Environmental Science and Technology, University of Maryland, College Park, MD 20742

[2] U.S. Department of Agriculture-Agricultural Research Service, Hydrology and Remote Sensing Laboratory, Beltsville, MD 20705

[3] School of Engineering, the University of Newcastle, Callaghan NSW 2308, Australia

[4] Department of Geographical Sciences, University of Maryland, College Park, MD 20742

[5] U.S. Geological Survey, Eastern Geographic Science Center, Reston, VA 20192

[6] U.S. Fish & Wildlife Service, National Wetlands Inventory, Falls Church, VA 22041

[7] Department of Energy and Environment, Government of the District of Columbia, Washington, DC 20002

Abstract

Water quality problems in the Chesapeake Bay Watershed (CBW) are expected to be exacerbated by climate variability and change. However, climate impacts on agricultural lands and resultant nutrient loads into surface water resources are largely unknown. This study evaluated the impacts of climate variability and change on two adjacent watersheds in the Coastal Plain of the CBW, using the Soil and Water Assessment Tool (SWAT) model. We prepared six climate sensitivity scenarios to assess the individual impacts of variations in CO_2 concentration (590 and 850 ppm), precipitation increase (11 and 21 %) and temperature increase (2.9 and 5.0 °C), based on regional general circulation model (GCM) projections. Further, we considered the ensemble of five GCM projections (2085 – 2098) under the representative concentration pathway (RCP) 8.5 scenario to evaluate simultaneous changes in CO_2, precipitation and temperature. Using SWAT model simulations from 2001 to 2014, as a baseline scenario, predicted hydrologic outputs (water and nitrate budgets) and crop growth were analyzed. Compared to the baseline scenario, a precipitation increase of 21 % and elevated CO_2 concentration of 850 ppm significantly increased stream flow and nitrate loads by 50 % and 52 %, respectively, while a temperature increase of 5.0 °C reduced stream flow and nitrate loads by 12 % and 13 %, respectively. Crop biomass increased by elevated CO_2 concentrations due to enhanced radiation- and water-use efficiency, while it decreased by precipitation and temperature increases. Over the GCM ensemble mean, annual stream flow and nitrate loads showed an increase of ~ 70 %, relative to the baseline scenario, due to elevated CO_2 concentrations and precipitation increase. Different hydrological responses to climate change were observed from the two watersheds, due to contrasting land use and soil characteristics. The watershed with larger percent croplands indicated a greater increase rate of 5.2 kg N ha^{-1} in nitrate yield relative

to the watershed with less percent croplands as a result of increased export of nitrate derived from fertilizer. The watershed dominated by poorly-drained soils showed increased nitrate removal due do enhanced denitrification compared to the watershed dominated by well-drained soils. Based on our findings, it is suggested that increased implementation of conservation practices would be necessary for this region to mitigate increased nitrate loads associated with predicted changes in future climate.

1 Introduction

Located in the Mid-Atlantic region, the Chesapeake Bay (CB) is the largest and most productive estuary in the United States (US). The Chesapeake Bay Watershed (CBW) covers an area of 166,000 km^2 and is home to more than 18 million people and 3,600 species of plants and animals (Chesapeake Bay Program, 2016). Despite significant restoration efforts, the health of the Bay has continued to deteriorate, primarily due to excessive nutrients and sediment loadings from agricultural lands (Rogers and McCarty, 2000). Najjar et al. (2010) suggested that the current water quality problems in the Bay are expected to worsen under climate variability and change. General Circulation Models (GCMs) have projected increases in temperature and precipitation of up to 5.0 °C and 21 %, respectively, by the end of this century in the CB region (Najjar et al., 2009), which could lead to substantial changes in the hydrology and nitrogen (N) cycling. For instance, Howarth et al. (2006) reported that greater precipitation is anticipated to increase N loads to the CB by ~ 65 %. With precipitation and temperature changes, elevated CO_2 concentrations affecting stomatal conductance has also been viewed as one of decisive factors modifying watershed hydrological processes (Chaplot, 2007; Wu et al., 2012a and 2012b).

Numerous studies have been conducted to demonstrate the impacts of changes in CO_2 concentrations, precipitation, and temperature on stream flow and N loads. Elevated CO_2 concentrations are predicted to increase stream flow by reduction of evapotranspiration (ET) that results from a decrease in plant stomatal conductance (Field et al., 1995; Jha et al., 2006; Wu et al., 2012a and 2012b). Jha et al. (2006), for example, showed that a doubling of CO_2 concentration increased water loads by ~ 36 % in the upper Mississippi river basin. Precipitation increase/decrease was found to directly cause the rise/fall of stream flow levels (Jha et al., 2006; Ficklin et al. 2009; Wu et al., 2012a; Praskievicz, 2014; Uniyal et al., 2015). Similarly, the study

by Ficklin et al. (2009) found that precipitation change of + 20 % and – 20 % led to changes in water loads by nearly + 17 % and – 14 %, respectively, in the San Joaquin River watershed, California. Temperature increase was reported to reduce stream flow during summer seasons due to the intensified ET values, but to increase stream flow during winter seasons due to an upsurge of snow melting (Jha et al., 2006; Ficklin et al. 2009 and 2013; Wu et al., 2012a; Praskievicz, 2014). Interestingly, in most studies, the responses of N loads to climate variability were found to be similar to the response of stream flow (Ficklin et al. 2009; Wu et al., 2012a; Praskievicz, 2014; Gombault et al., 2015). According to the projected climatic conditions (e.g., elevated CO_2 concentrations, precipitation and temperature increases) illustrated in Najjar et al. (2009), substantial variations in stream flow and N loads are anticipated in the CBW. Therefore, it is important to investigate potential climate change impacts on watershed hydrological processes to efficiently mitigate water quality degradation.

However, climate change impacts on hydrological processes have not been fully investigated in the CBW region. Howarth et al. (2006) attempted to quantify N loads under modified climate conditions, but their projections relied on the statistical relationships between river discharge/precipitation and N loads. Lee et al. (2015) predicted changes in stream flow and nitrate loads at the outlet of the watershed in response to climate variability (e.g., elevated CO_2 concentrations, precipitation and temperature increase). To cope with climate change-driven modifications, it is imperative to have an understanding of a wide range of changes in hydrological processes (Najjar et al., 2010). A simple projection of aggregated watershed responses (water quality variables at the outlet of the watershed) would be limited to suggest conservation practices to reduce climate change impacts. Understanding of internal watershed processes (i.e., water and nutrient transport mechanisms) within a watershed can guide site-

specific management plan to aid conservation decision making. In addition, climate impacts on agriculture is extremely important for the CB region because agriculture is the single largest nutrient source and modified crop growth by climate change can exert great impacts on internal watershed processes (Najjar et al., 2010). However, previous studies did not fully demonstrate climate change impacts on internal watershed processes considering detailed agricultural management practices.

Moreover, responses of watershed hydrological processes to climate variability and change can vary by watershed characteristics (e.g., land use and soil drainage conditions). For example, several studies showed that watersheds with a greater area of cropland released a higher amount of nitrate than areas with less cropland, mainly due to agricultural N inputs (Jordan et al., 1997; Hively et al., 2011; McCarty et al., 2014). Thus, climate change can lead to greater nitrate export from watersheds with a larger percent cropland area, due to increased export of N from fertilizer application. Additionally, different soil characteristics also can lead to different responses in watershed-scale water and N cycles under climate change. A study by Chiang (1971) showed that well-drained soils with a high infiltration rate promote water percolation, increasing groundwater contribution to stream flow. Nitrate leaching is also found to frequently occur in well-drained soils (Lee et al., 2016a). In contrast, poorly-drained soils with a low infiltration rate provide anaerobic conditions favorable to denitrification, resulting in nitrate removal in soils and groundwater (Denver et al., 2010; Lee et al., 2016a; Sharifi et al., 2016). For example, prior converted croplands, which are also known as "currently farmed historical wetlands", often associated with poorly-drained soil were also shown to have prominent impacts on reducing agrochemical loadings in the CBW region during the winter season, when ET is low which results in a higher groundwater table (Tiner and Burke, 1995;

Denver et al., 2014; McCarty et al., 2014; Sharifi et al., 2016). Artificial drainage systems in agricultural lands are widely developed on poorly-drained soils in this region, resulting in an increase of water and nutrient transport from lands to nearby streams through surface runoff (McCarty et al., 2008; Fisher et al., 2010). Therefore, water and nitrate fluxes in the watersheds with different soil characteristic are expected to show distinctive responses to climate variability and change.

This study aimed at evaluating the impacts of potential climate variability and change on water and nitrate budgets in two adjacent watersheds on the Coastal Plain of the CBW, using the Soil and Water Assessment Tool (SWAT) model. This process-based water quality model has been widely used to predict climate change impacts on numerous watersheds (Gassman et al., 2007; Uniyal et al., 2015). We prepared six climate sensitivity scenarios to assess the individual impacts of changes in CO_2 concentration (590 and 850 ppm), precipitation (11 and 21 %) and temperature (2.9 and 5.0 °C) increase. This sensitivity analysis was prepared to develop in-depth knowledge and understanding on how each climate factor affects internal watershed processes and crop growth. Then, the simulations with five GCM projections (referred to as the GCM scenario) was conducted to evaluate watershed internal processes and crop growth under foreseeable climate conditions that considers simultaneous changes in CO_2, precipitation and temperature. We used the GCM projections to describe foreseeable changes, as the combination of climate factors and their interactions could not provide complete climate change/variability information including seasonal and inter-decadal variability (Mearns, 2001). We first assessed climate change impacts on water and nitrate loadings by analyzing internal watershed processes and crop growth, and then, comparative analyses between two watersheds were conducted to identify critical landscape characteristics that affected nitrate loads. Finally, suggestions were

provided regarding conservation practice implementation to improve the resilience of coastal watersheds to the future climate change in the CBW region.

2 Materials and Methods

2.1 Study area

This study was undertaken on two adjacent watersheds, Tuckahoe Creek Watershed (TCW, ~220.7 km^2) and Greensboro Watershed (GW, ~290.1 km^2). They are sub-watersheds of the Choptank River Watershed located in the Coastal Plain of the CBW (Figure 1). The Choptank River Watershed is one of the Conservation Effects Assessment Project (CEAP) Benchmark watersheds of the US Department of Agriculture (USDA)-Natural Resources Conservation Service (NRCS). The US Environmental Protection Agency (USEPA) has listed this watershed, as "impaired" under Section 303(d) of the 1972 Clean Water Act, primarily due to the excessive nutrient and sediment loadings (McCarty et al. 2008). The two adjacent sub-watersheds have distinctive characteristics considering the distribution of land use and soil drainage conditions (Figure 2 and Table 1). The TCW is dominated by agricultural lands (54 %) and forest (32.8 %) with well-drained soils, classified as hydrologic soil groups (HSG) – either A or B. These soils account for 56% of the total watershed and 69.5 % of the agricultural lands (Figure 2). Thus, water and nitrate fluxes tend to be easily percolated and leached into soils and groundwater, and thus groundwater flow is considered as a major water pathway for nutrient fluxes to streams in the TCW (Lee et al., 2016a). In comparison, forest (48.3 %) is the major land use type in the GW, followed by agricultural (36.1 %). Soils that are poorly-drained (HSG

– C or D) occupy 75 % of the total area and 67.2 % of agricultural lands, which result in a low infiltration and high denitrification.

[Insert Figure 1. The location of Tuckahoe Creek Watershed (left) and Greensboro Watershed (right)]

[Insert Figure 2. The physical characteristics of the Tuckahoe Creek Watershed (left) and Greensboro Watershed (right); (a) land use, (b) hydrologic soil groups, and (c) elevation]

[Insert Table 1. Soil properties and land use distribution of the Tuckahoe Creek Watershed (TCW) and Greensboro Watershed (GW)]

2.2 Soil and Water Assessment Tool (SWAT)

The SWAT is a process-based watershed model, developed to assess the impact of human activities and land use on water and nutrient cycles within agricultural watersheds (Netisch et al., 2011). The SWAT divides a watershed into sub-watersheds using a Digital Elevation Model (DEM), and each sub-watershed is further divided into hydrological response units (HRUs) based on a unique combination of land use, soil type, and slope. Model simulation is performed at the HRU level, and the simulated outputs aggregated at the sub-watershed and then further at the watershed level through routing processes. The amount of surface runoff and infiltration are calculated based on Soil Conservation Service (SCS) Curve Number (CN) method, and the CN values are updated daily based on soil permeability, land use type, and antecedent soil water conditions. Water infiltrated into soils is either delivered to streams through lateral flow or further percolated into groundwater, when soil water content exceeds its field capacity. The groundwater portion is then either transported to streams through groundwater flow, percolated

into the deep groundwater aquifer, or discharged to the soil profile. The amount of nitrate in soils increases by nitrification, mineralization of soil organic and crop residue, biological N fixation, and fertilization, but it decreases through denitrification and plant uptake (Neitsch et al., 2011). Nitrate fluxes move via surface runoff, lateral flow, percolated water from soil to groundwater, and groundwater flow. Nitrate concentration in the mobile water (i.e., surface runoff, lateral flow, and percolated water) is first determined and then nitrate fluxes in the mobile water is calculated based on the nitrate concentration and the amount of mobile water. Nitrate in groundwater is re-distributed in four ways: remain in the groundwater, recharge to deep groundwater, move to streams, or discharge to the soils. Nitrate removal by biological and chemical processes in groundwater is simulated by the first-order kinetics. Refer to Netisch et al. (2011) for further details.

The SWAT model has the capability of simulating the impacts of CO_2 concentration on ET and biomass accumulations. The Penman-Monteith method used for this study considers CO_2 effects on ET based on the relationship between plant stomatal conductance and CO_2 concentration:

$$g_{l,CO_2} = g_l \times [1.4 - 0.4 \times (CO_2 / 330)] \quad (1)$$

where g_{l,co_2} is the leaf conductance modified to reflect CO_2 effects, and g_l is the leaf conductance without the effect of CO_2. The equation shows the linear reduction of the leaf conductance with increasing CO_2 and results in 40 % reduction in leaf conductance for all plants when CO_2 concentration is doubled. According to Eq. (1) elevated CO_2 concentrations decrease plant stomatal conductance and canopy resistance, subsequently reducing ET. Refer to Neitsch et al. (2011) for details on the Penman-Monteith method.

The simulation of the crop growth in the SWAT is based on potential heat unit theory. The model considers the impacts of CO_2 concentration on crop biomass growth by modifying radiation-use efficiency (RUE) of the plant as follows:

$$RUE = \frac{100 \cdot CO_2}{CO_2 + \exp(r_1 - r_2 \cdot CO_2)} \quad (2)$$

where RUE is radiation-use efficiency of a plant, and r_1 and r_2 are coefficients.

$$\Delta bio = RUE \cdot H_{phosyn} \quad (3)$$

where Δbio is a potential increase in plant biomass on a given day and H_{phosyn} is the amount of intercepted photosynthetically active radiation on a given day.

2.3 Baseline SWAT input data

Climate and geospatial data needed for the SWAT simulation are summarized in Table 2. Daily precipitation and temperature were obtained from three meteorological stations operated by the National Oceanic and Atmospheric Administration (NOAA) National Climate Data Center (NCDC) at Chestertown, Royal Oak, and Greensboro (USC00181750, USC00187806, and US1MDCL0009, respectively). Due to data unavailability, humidity, wind speed, and solar radiation were generated using the SWAT built-in weather generator (Neitsch et al., 2011). Monthly stream flow data were downloaded from US Geological Survey (USGS) gauge stations on the Tuckahoe Creek near Ruthsburg (USGS#01491500) and the Choptank River near Greensboro (USGS#01491000) (Figure. 1). The USGS LOAD ESTimator (LOADEST, Runkel et al. (2004)) was used to generate continuous monthly nitrate loads from nitrate grab sample

241 data (133 samples over the simulation period) that were obtained from the Chesapeake Bay
242 Program (CBP, TUK#0181) for the TCW, and obtained from USGS gauge station data
243 (USGS#01491000) for the GW. The LOADEST is used commonly to generate continuous data
244 from discrete data and it was shown to accurately generate water quality variables (Jha et al.,
245 2013; Lee et al., 2016b). The land use and soil maps, and DEM were prepared as shown in Table
246 2.

247 [Insert Table 2. List of the SWAT model input data]

248 We identified representative agricultural practices for this region using multiple
249 geospatial data (Lee et al., 2016a). Major crop rotations and their year to year placement was
250 derived through analysis of the USDA-National Agricultural Statistics Service (NASS) Cropland
251 Data Layer (CDL) for the period of 2008 – 2012. We assumed that crop rotation and land use
252 did not change over the simulation period so that agricultural N input did not vary for the
253 baseline and GCM scenarios. Detailed agricultural management information (e.g., the amount,
254 type, and application timing of fertilizer, and planting and harvesting timings of individual crops)
255 was developed through literature review and communications with local experts (Table A1).
256 Detailed information about the development of crop rotation and land management is available
257 in Lee et al. (2016a).

258

259 **2.4 Baseline SWAT calibration and validation**

260 The SWAT model runs were performed at a monthly time step for 16 years; these include
261 a 2-year warm-up (1999 – 2000), 8-year calibration (2001 – 2008), and 6-year validation period
262 (2009 – 2014). The SWAT model was simulated at a daily time step based on daily climate

input, and daily outputs were aggregated to monthly outputs. It should be noted that due to unavailability of observations before 2001, model calibration and validation were initiated from 2001. Compared to past 30-year precipitation data (1981 - 2010), climate condition over the calibration period (2001 - 2008) was shown to include representative wet, dry, and average climate conditions while the validation period (2009 - 2014) was dominated by wet conditions. Critical parameters used for model calibration were selected based on previous studies conducted in this region (Sexton et al., 2010; Yeo et al., 2014; Lee et al., 2016a) and allowable ranges of these parameters were derived from literature presented in the caption of Table 3. Stream flow parameters were manually calibrated and then nitrate parameters were adjusted following SWAT calibration guideline (Arnold et al., 2012). A set of parameters, that produced the best model performances and fulfilled model performance criteria suggested by Moriasi et al. (2007), were chosen for model validation. Model performance was evaluated using the following statistics: Nash-Sutcliffe Efficiency coefficient (NSE), Root Mean Square Error ($RMSE$)-Standard deviation Ratio (RSR), and Percent bias ($P-bias$).

$$NSE = 1 - \left[\frac{\sum_{i=1}^{n} (O_i - S_i)^2}{\sum_{i=1}^{n} (O_i - \bar{O})^2} \right] \quad (4)$$

$$RSR = \frac{RMSE}{STDEV_{obs}} = \frac{\left[\sqrt{\sum_{i=1}^{n} (O_i - S_i)^2} \right]}{\left[\sqrt{\sum_{i=1}^{n} (O_i - \bar{O})^2} \right]} \quad (5)$$

$$P-bias=\left[\frac{\sum_{i=1}^{n}(O_i-S_i)\times 100}{\sum_{i=1}^{n}O_i}\right] \quad (6)$$

where O_i is the observed data at time step i, and S_i is the simulated output at time step i, $\overline{O}$ is the mean of observed data over all time steps, and n is the total number of observed data. We also calculated NSE for the natural logarithm of stream flow to evaluate model performance for low-flows (Kiptala et al., 2014). In addition, the 95 percent prediction uncertainty (95 PPU) band was represented to evaluate model uncertainty (Singh et al., 2014). The 95 PPU was computed based on all simulated outputs generated during the calibration process. The 95 PPU was represented as the range of values between the 2.5 and 97.5 percentiles of the cumulative distribution of simulated outputs.

[Insert Table 3. List of calibrated parameters]

2.5 Climate sensitivity and GCM scenarios

To evaluate the impacts of climate variability and change on watershed hydrological processes, climate sensitivity and GCM scenarios were prepared as illustrated below (see 2.5.1 and 2.5.2). The calibrated SWAT model was simulated using the climate sensitivity and GCM scenarios for comparison with baseline water and nitrate budgets.

2.5.1 Climate sensitivity scenarios

297 A climate sensitivity analysis aids in identifying the degree or threshold of responses of
298 hydrologic variables to climate-induced modifications and a sensitivity scenario generally
299 assumes constant changes throughout the year (Mearns, 2001). Following the approach in
300 Mearns (2001), six climate sensitivity scenarios were prepared by modifying the baseline data
301 (1999 – 2014) to assess individual effects of elevated CO_2 concentrations, precipitation and
302 temperature on watershed hydrological processes (Table 4). Sensitivity scenarios were designed
303 to change one variable while holding other variables constant throughout the simulations.
304 Baseline precipitation and temperature were modified by percent and absolute changes using
305 anomaly and absolute data, respectively, as illustrated in Najjar et al. (2009). They reported
306 mean temperature and precipitation changes over the CB for three future periods (2010 – 2039,
307 2040 – 2069, and 2070 – 2099) relative to the baseline period (1971 – 2000) based on GCM
308 outputs (Najjar et al., 2009). We used the maximum increase rate (and value) for 2040 – 2069
309 (precipitation: 11 % and temperature: 2.9 °C) and 2070 – 2099 (precipitation: 21 % and
310 temperature: 5.0 °C) to set the precipitation and temperature sensitivity scenarios. For example,
311 baseline precipitation increased by 11 % and 21 % for Scenario 3 and 4, respectively, and 2.9 °C
312 and 5.0 °C were added to the baseline temperature for Scenario 5 and 6, respectively (Table 4).
313 Baseline CO_2 concentration was set as the default value (330 ppm) for simulations. For the first
314 and second scenarios, baseline CO_2 concentration was replaced with 590 and 850 ppm,
315 respectively. The upper value of 850 ppm was used because GCMs used for temperature and
316 precipitation sensitivity scenarios were forced with the assumption of CO_2 concentration of 850
317 ppm (Najjar et al., 2009). The lower value of 590 ppm (the average of 330 and 850 ppm) was
318 considered to be the level of CO_2 concentration around the middle of this century.

319 [Insert Table 4. Climate sensitivity scenarios developed by modifying baseline values]

2.5.2 GCM scenario

A GCM-based scenario is the most commonly used method for assessing future climate change impacts (Mearns, 2001). We downloaded projected climate data (e.g., daily precipitation and maximum and minimum temperature) from the World Climate Research Program's (WCRP's) Coupled Model Intercomparison Project5 (CMIP5) archive (Brekke et al., 2013). Five GCM data under the representative concentration pathway (RCP) 8.5 scenario were downloaded (Table A2), because the RCP 8.5 indicates the highest value of CO_2 concentration in the CMIP5. To be consistent with the period of the baseline data (1999 – 2014), 16-year future data (2083 – 2098) were used in this study. We further refined GCM data using the delta change method because spatially downscaled data are consistent with historical observations at the global scale, but could be significantly inconsistent at fine spatial scales, such as a watershed (Wang et al., 2014). The delta change method was calculated as follows:

$$P_{delta} = GCM_{P-future,monthly} \div GCM_{P-baseline,monthly} \quad (7)$$

$$T_{delta} = GCM_{T-future,monthly} - GCM_{T-baseline,monthly} \quad (8)$$

$$DGCM_{P-future,dailly} = OBS_{P-baseline,daily} \times P_{delta} \quad (9)$$

$$DGCM_{T-future,dailly} = OBS_{T-baseline,daily} + T_{delta} \quad (10)$$

where, P_{delta} and T_{delta} indicate precipitation ($_P$) and temperature ($_T$) biases in GCM data, respectively, $GCM_{future,monthly}$ and $GCM_{baseline,monthly}$ indicate the monthly average of GCM data for the future (2083 - 2098) and baseline (1999 - 2014) periods, respectively, $OBS_{baseline,daily}$ indicates observed daily climate, and $DGCM_{future,dailly}$ indicates unbiased

future climate data. We calculated the ensemble mean of delta-change values from the five GCMs, because substantial variations existed among the GCM projections (Shrestha et al., 2012; Van Liew et al., 2012). Then, the SWAT model was simulated using the ensemble mean to predict hydrological processes under future climate conditions. Similar to the baseline scenario, humidity, wind speed, and solar radiation values were generated using the SWAT built-in weather generator owing to data unavailability. We assumed CO_2 concentration for the GCM scenario at 936 ppm, as specified CO_2 concentration under the RCP8.5 scenario (Meinshausen et al., 2011).

2.6 Analyses of simulation outputs

Simulated outputs were summarized at multiple temporal scales (e.g., monthly, seasonal, and annual). Annual averages of stream flow, ET, and nitrate loads were calculated to investigate changes in water and nitrate budgets in response to climate sensitivity and GCM scenarios. The response of crop growth to climate variability and change was also analyzed to show the effects of modified crop biomass on hydrology and N cycle. For comparative analyses between two watersheds, water and nitrate yields were summarized seasonally for climate sensitivity scenarios (i.e., summer (April – September) and winter (October – March)) and monthly for the GCM scenario. Note that water and nitrate yields indicate the summations of water and nitrate fluxes transported from lands to streams by surface runoff, lateral flow, and groundwater flow. All simulation outputs were normalized by total watershed size.

We conducted a statistical analysis to test if the simulation results under climate sensitivity and GCM scenarios were statistically different from those under the baseline scenario using parametric (paired t-test) and nonparametric (Wilcoxon signed rank) methods. Note that

363 we used monthly outputs (168 samples over 14 years) for this analysis. The statistical
364 significance for the difference was indicated by *p-value*.

365

366 **3 Results and Discussions**

367 **3.1 Model calibration and validation**

368 Monthly simulations for stream flow and nitrate loads were compared with corresponding
369 observations (Figure 3). Results show that simulated monthly stream flow were in good
370 agreement with observations, but simulated peak stream flows were underestimated relative to
371 observations. This underestimation was attributed to the inherent limitations of the SWAT
372 model and limited climate data to capture local storm effects as it does not account for intensity
373 and duration of the precipitation (Qiu et al., 2012). Previous studies conducted in this region
374 showed similar results, though the overall simulation results accurately replicated the
375 observations (Yeo et al., 2014; Lee et al., 2016a). Simulated nitrate loads were also well
376 matched with actual observations and the uncertainty band (shown as green in Figure 3) captured
377 most observations in the two watersheds. Overall, model performance measures fulfilled "good"
378 (e.g., $0.65 < NSE \leq 0.75$) or "very good" ($0.75 < NSE$) criteria for stream flow and at least
379 "satisfactory" ($0.5 < NSE \leq 0.65$) for nitrate loads (Table 5). The model performance measures
380 for low-flows (NSE for the natural logarithm of stream flow) also indicated "satisfactory" to
381 "very good" (Table 5). These results demonstrated that the calibrated model replicated actual
382 conditions reasonably well (Moriasi et al., 2007; Arnold et al. 2012).

383 [Insert Figure 3. Simulated and observed monthly stream flow and nitrate loads for (a & b) TCW
384 and (c & d) GW during calibration and validation periods]

[Insert Table 5. Model performance measures for monthly stream flow and nitrate loads]

3.2 Responses to climate sensitivity scenarios

3.2.1 Water and nitrate budgets

14-year averages of annual hydrologic variables under the baseline and climate sensitivity scenarios are presented in Figure 4. Elevated CO_2 concentrations (590 and 850 ppm) and precipitation increase (11 and 21 %) led to significant increases in annual stream flow and nitrate loads by 50 % and 52 % for the TCW and 43 % and 33 % for the GW, respectively, relative to the baseline scenario (*p-value* < 0.01) (Figure 4). Elevated CO_2 concentrations lowered plant's stomatal conductance, resulting in a decrease in ET of 30 % and thereby increased stream flow and corresponding nitrate loads (Figure 4). The reduced rate of ET (driven by CO_2 concentrations of 850 ppm) demonstrated in this study is supported by previous studies using SWAT, such as Ficklin et al., 2009 (- 40 %; 970 ppm) and Pervez et al., 2015 (- 12 %; 660 ppm). Precipitation increase resulted in a direct increase in stream flow, leading to increased nitrate loads. Compared to the baseline scenario, a temperature increase of 5 °C significantly reduced annual stream flow and nitrate loads by 12 % and 13 % for the TCW and 11 and 13 % for the GW (*p-value* < 0.01), respectively, due to intensified ET (Figure 4).

It should be noted that the standard version of SWAT tends to overestimate the impact of CO_2 on reduction of ET (Eckhardt and Ulbrich, 2003). Maximum leaf area index (LAI) is assumed to be constant regardless of variation in CO_2 concentration in SWAT. However, maximum LAI is known to increase with increasing CO_2 concentration (Eckhardt and Ulbrich, 2003). In addition, the degree of reduction in stomatal conductance varies by plant species, which also is not taken into account in the SWAT model. Another model simplification, which increases uncertainty, is the application of the same reduction rate to all plants. For example, C3

crops (soybean and wheat) are known to have less reduction in stomatal conductance with rising CO_2 concentration compared to C4 crops (corn) (Ainsworth and Rogers, 2007). Both factors could contribute to overestimating reduction of ET and resultant increase in stream flow and nitrate loads (Eckhardt and Ulbrich, 2003).

Changes in crop growth under climate sensitivity scenarios had great impacts on water and nitrate budgets. Although precipitation increase resulted in the greatest increase in annual stream flow, annual nitrate loads were greater under elevated CO_2 concentrations (Figure 4ab), due to increased crop biomass and high N availability from mineralization of crop residues (Figure 5a). Elevated CO_2 concentrations stimulated crop growth by decreasing water demand and increasing radiation-use efficiency (Abler and Shortle, 2000; Parry et al., 2004). For example, simulated corn and soybean biomass increased from 1.5 and 0.9 Mg ha^{-1} (baseline concentration of 330 ppm) to 1.6 and 1.3 (CO_2 concentration of 850 ppm) Mg ha^{-1}, respectively (Figure 5a). Increased crop biomass left greater amounts of crop residue after harvesting crops (winter seasons: Oct. – Mar.), which contributed to increasing nitrate in soils through mineralization (Lee et al., 2016a). Our simulation results indicated that mineralized nitrate under elevated CO_2 concentrations increased by 27 % for the TCW and 23 % for the GW during winter seasons, compared to the baseline values (Figure A3). Increased crop residue resulted in greater nitrate loads under elevated CO_2 concentrations than under conditions of increased precipitation. In contrast, temperature increase led to lower crop biomass than the baseline value, due to increased heat stress (Figure 5c). Lower biomass reduced remaining crop residue and subsequently reduced mineralized nitrate by 22 % during winter seasons, compared to the baseline value (Figure A3). Reduction of mineralized nitrate contributed to decreased nitrate loads in conjunction with intensified ET. Precipitation increase slightly decreased corn biomass

because increased precipitation reduced the availability of nutrients for crops (Figure 5b), leading to increased nutrient stress. However, soybean biomass did not change in response to precipitation increase (Figure 5e) since soybean crops can generate N through fixation as needed.

[Insert Figure 4. 14-year average of annual hydrologic variables under the baseline and climate sensitivity scenarios at the watershed scale]

[Insert Figure 5. The responses of crop biomass growth to the climate sensitivity scenario: (a, b, and c) corn and (d, e, and f) soybean.]

3.2.2 Comparative analyses

For the purpose of comparing the two watersheds in response to climate sensitivity scenarios, 14-year averages of seasonal water and nitrate yields were calculated (Figure 6). Both elevated CO_2 concentrations and precipitation increase led to greater water and nitrate yields for the two watersheds during winter and summer seasons, compared to the baseline scenario. However, the seasonal pattern of nitrate yield differed between the two watersheds. Wintertime water yield was greater than summertime value for both watersheds, which was consistent with the seasonal pattern of nitrate yield for GW. However, summertime nitrate yield increases were greater than wintertime value for the TCW, apparently due to the difference in percent agricultural lands between the TCW (54.0 %) and GW (36.1 %). Increased water yield could accelerate the export of nitrate added to the watersheds through fertilizer activities mainly occurred during summer seasons. Accordingly, increased water yield caused by elevated CO_2 concentrations and precipitation increase induced considerable increase in summertime nitrate

yield by ~ 62.5 % for the TCW, while moderately increasing it by ~ 35.6 % for the GW, which is dominated by forest instead of croplands.

[Insert Figure 6. 14-year average of seasonal hydrologic variables under the baseline and climate sensitivity scenarios at the watershed scale]

Temperature increase reduced summertime water and nitrate yields by 18.5 % and 27 % for the TCW and 13.9 % and 20.2 % for the GW, respectively, mainly due to increased water loss by ET (Table A4). Wintertime water yield also decreased for the two watersheds, but changes in wintertime nitrate yield differed between the two watersheds. A decrease of 9.5 % in wintertime nitrate yield was found for GW, but wintertime nitrate yield increased by 1.6 % for the TCW (Figure 6b), due to modified crop growth patterns and contrasting soil characteristics between the two watersheds. Temperature increase could drive crops to reach maturity earlier while exerting increased heat stress on crops, leading to lower biomass compared to the baseline (Figure 5cf). These two factors collectively reduced soil water and nitrate consumption by crops at the end of the growth stage, subsequently increasing soil water content and nitrate leaching compared to the baseline (Figure A5). Nitrate leached into groundwater was discharged to streams through groundwater flow during winter seasons. The TCW showed increased nitrate leaching of 1.0 kg N ha^{-1} compared to GW, due to a larger percentage of well-drained soils with a high infiltration rate. Different leaching rates between the TCW and GW soils led to a greater increase in wintertime nitrate flux transported by groundwater flow (NGWQ) for the TCW (0.21 kg N ha^{-1}) compared to the GW (0.16 kg N ha^{-1}) (Figure 6b). However, intensified ET reduced wintertime water and nitrate fluxes transported by surface runoff (SURQ and NSURQ, respectively) for the two watersheds (Table A4) while water fluxes transported by lateral and groundwater flow (LATQ and GWQ, respectively) were rarely changed. Because the majority

476 of water flux was transported by groundwater flow for the TCW and surface runoff for the GW
477 (Figure 6a), a decrease in SURQ led to a substantial reduction of wintertime NSURQ for GW
478 (0.45 kg N ha^{-1}) and less reduction for the TCW (0.12 kg N ha^{-1}), compared to the baseline
479 (Figure 6b). Therefore, both increased NGWQ and decreased NSURQ during winter seasons
480 collectively led to an increasing pattern of wintertime nitrate yield for the TCW and a decreasing
481 pattern for the GW, compared to the baseline scenario. Note that denitrification was rarely
482 affected by temperature increase because reduced soil water content by increased ET through
483 higher temperatures decreased denitrification.

484

485 **3.3 Responses to the GCM scenario**

486 **3.3.1 Comparison of climate data**

487 The monthly averages of mean temperature and cumulative precipitation under the
488 baseline scenario were compared with the ensemble means of five GCMs (Figure 7). Projected
489 temperature was constantly higher than the baseline value throughout the year by 3.8 – 6.2 °C
490 (Figure 7a). Compared to the baseline, projected precipitation was greater except for March and
491 October. (Figure 7b). Monthly cumulative precipitation was up to 19 mm greater on August and
492 up to 11 mm lower on October, in comparison to the baseline values. Note that the annual
493 average of mean temperature increased from 13.9 °C (baseline) to 18.6 °C (projection), and the
494 annual average of cumulative precipitation also increased from 1221 mm (baseline) to 1322 mm
495 (projection).

496 [Insert Figure 7. Monthly average of (a) mean temperature and (b) cumulative precipitation for
497 the baseline (2001 – 2014) and future (2085 – 2098) periods]

3.3.2 Water and nitrate budgets

Baseline hydrologic variables (e.g., stream flow, ET, and nitrate loads) are compared with the simulated outputs in Table 6. Relative to the baseline scenario, annual stream flow and nitrate loads significantly increased by 70 % and 66 % for the TCW and 50 % and 56 % for the GW, respectively (*p-value* < 0.01). These increasing patterns were mainly caused by two factors: 1) increased precipitation and 2) decreased ET resulting from elevated CO_2 concentration of 936 ppm. Annual precipitation increased by 8 % and elevated CO_2 concentrations reduced ET by 32 % for the TCW and 26 % for the GW (Table 6).

[Insert Table 6. 14-year average of hydrologic variables under the baseline and GCM scenarios]

3.3.3 Comparative analyses

Responses of the two watersheds to the GCM scenario were compared using the monthly averages of water and nitrate yields in Figure 9. Relative to the baseline, projected water and nitrate yield was greater over the year. The greatest increase in water yield was observed on August and September when the increase rate of precipitation was greatest. However, the increase rate of nitrate yield was higher on April than other months, due to a significant export of nitrate from fertilizer applications.

An increase rate of nitrate yield (under the GCM scenario relative to the baseline scenario) was 5.2 kg N ha^{-1} greater in the TCW compared to the GW, mainly due to two watershed characteristics (Figure 9cd). First, a larger percentage of croplands in TCW led to greater nitrate export from fertilizer application compared to GW with smaller percent croplands. This was because increased water yield by elevated CO_2 concentrations and precipitation increase

promoted the export of nitrate in soil profile (Suddick et al., 2013). For example, nitrate yield increased by 1.4 kg N ha^{-1} for the TCW and 0.9 kg N ha^{-1} for the GW in April, when fertilizer application occurred, compared to the baseline. Second, a larger percentage of poorly-drained soils in the GW contributed to reducing nitrate yield via greater potential of denitrification, compared to the TCW dominated by well-drained soils, under the GCM scenario. Increased soil water content resulting from elevated CO_2 concentration of 936 ppm provided anaerobic conditions for denitrification. Compared to the baseline, the GW and TCW showed increased nitrate (removed by denitrification) of 3.9 and 0.5 kg N ha^{-1} under the GCM scenario, respectively. Eventually, GW lost 8.7 kg N ha^{-1} more nitrate flux via denitrification than the TCW, which likely led to lowering nitrate yield for the GW.

[Insert Figure 8. 14-year average of monthly water and nitrate yields under the baseline and GCM scenarios]

4 Implications and limitations

The key results of this study can suggest important future research for improving our understanding of climate change impacts on nutrient loads into the CBW. Analysis of climate variability and change impacts on watershed hydrological processes illustrated the close relationship between agricultural activities and future nitrate export in the watershed dominated by croplands, due to excessive export of nitrate from springtime fertilizer application. Changes in crop growth are likely to alter current agricultural activities and associated nitrate loads. Fertilizer application might increase in the future because increased extreme climate conditions (e.g., high intensity rainfall and flooding) might lead to increased risk of nutrient loss to leaching and runoff, reducing the fertilizer use efficiency of field crops (Suddick et al., 2013). Our

simulation also indicated considerable increases in nitrate transported by surface runoff (NSURQ) due to increased precipitation on April, when the vast majority of fertilizers were applied (Figure 8bd). As a result, projected corn biomass appeared to be 0.03 Mg ha^{-1} lower than the baseline value, likely due to increased nutrient stress (Figure 9a). However, soybean biomass increased under the GCM scenario since soybean could accumulate N through biological fixation and elevated CO_2 concentrations contributed to biomass growth (Figure 9b). To adapt to warmer temperatures, early planting of summer crops could be suggested to increase crop production while reducing heat stress (Woznicki et al., 2015). For example, when planting dates were shifted 10 days earlier, soybean yield increased on average of 0.03 Mg ha^{-1} (Figure 8b). Contrary to our expectation, corn yield decreased under the earlier planting date, due to increased nutrient stress resulting from intensified precipitation. Lastly, irrigation patterns could be changed due to decreased ET under elevated CO_2 conditions. However, there are limited studies investigating future agricultural practices. Therefore, it is crucial to investigate potential agricultural activities under climate change and their effects on nitrate loads.

[Insert Figure 9. Crop biomass growth and stress under the baseline and GCM scenarios: (a) corn and (b) soybean]

Climate change-driven modifications indicated a potential overall increase in nitrate export. Therefore, the importance of conservation practices aimed at N mitigation would be even more critical in the future. Comparative analyses of two watersheds can provide practical guideline and have implications for agricultural watersheds on coastal areas in the CBW because our analyses considered climate change impacts on croplands (crop growth, water and nutrient cycling) and their transport mechanisms with detailed agricultural management practice. In addition, the two watersheds showed the typical site characteristics in the coastal watershed, in

terms of topographic and soil characteristics, and the agricultural practices commonly used in the CBW. Hence, the findings from this study can be applicable to other catchments in the CBW region and will be useful to prepare climate change adaptation strategies. For example, the control of nutrients in manure or fertilizer would be more critical for reducing nitrate export from a watershed dominated by croplands. Winter cover crops, which are widely implemented in this region, would likely show increased value in mitigating agricultural nitrate loss during winter seasons, considering increased N availability and increased wintertime precipitation. In a watershed dominated by poorly-drained soils, wetland restoration would be well positioned to enhance denitrification (McCarty et al., 2014), as would be the use of drainage control structures on ditches and tiles draining prior converted croplands (poorly drained areas of the farm landscape).

Note that although forest litterfall have significant impacts on nutrient cycles (Zhang et al., 2014), the current version of SWAT model is limited to represent those forest impacts (Yang et al., 2016). In our simulation, growth of deciduous tree was simulated at forest areas with the default setting. This setting allowed tree growth to affect water and nutrient cycling via ET and uptake, but simulated tree growth was considerably underestimated compared to actual growth and litterfall was rarely considered (Yang et al., 2016). Hence, our simulation might poorly represent the ecological responses of forests to climate change. Future work should accurately consider forest ecosystems through model improvement.

5 Summary and conclusion

Water quality degradation by human activities on agricultural lands is a great concern on the Coastal Plain of the CBW. This degradation is expected to worsen in the future due to changes

587 in climate variability and conditions. However, there is limited information about how climate
588 change will influence hydrology and nutrient cycles. This study used the SWAT model to
589 simulate the impacts of potential climate variability and change on two adjacent watersheds in
590 the Coastal Plain of the CBW. The climate sensitivity and GCM scenarios were prepared to
591 assess the individual and combined impact of three climate factors (e.g., increases in CO_2
592 concentration, precipitation, and temperature). We performed comparative analyses between
593 two watersheds to show how key landscape characteristics influence the watershed level
594 response to climate variability and change.

595 Our simulation results showed that water and nitrate budgets in two watersheds in the Coastal
596 Plain of the CBW were significantly sensitive to climate variability and change. Compared to
597 the baseline scenario, a precipitation increase of 21 % and elevated CO_2 concentrations of 850
598 ppm resulted in increases in stream flow and nitrate loads of 50 % and 52 %, respectively. A
599 temperature increase of 5.0 °C reduced stream flow and nitrate loads by 12 % and 13 %,
600 respectively. Under the GCM scenario, annual stream flow and nitrate loads increased by 70 %
601 and 66 %, respectively, compared to the baseline scenario. Contrasting land use and soil
602 characteristics led to different patterns of nitrate yield between two watersheds. The watershed
603 with a larger percent cropland indicated 5.2 kg N ha^{-1} greater increase rate of nitrate yield (under
604 the GCM scenario relative to the baseline scenario) compared to the one with less percent
605 croplands under the GCM scenario, due to increased export of nitrate derived from fertilizer.
606 Increased nitrate loss by denitrification also contributed to less increase in nitrate yield in the
607 watershed dominated by poorly-drained soils compared to the watershed dominated by well-
608 drained soils. Based on our results, we suggest that increased implementation of conservation
609 practices, such as nutrient management planning, winter cover crops, and wetland restoration and

enhancement, is necessary to mitigate increased nitrate loads by climate change. These findings may help watershed managers and decision makers to establish climate change adaptation strategies for mitigating water quality degradation in areas impaired by excessive agricultural nutrient loadings.

Acknowledgement

This research was supported by the US Department of Agriculture (USDA) Conservation Effects Assessment Project (CEAP), National Aeronautics and Space Administration (NASA) Land Cover and Land Use Change (LCLUC) Program (award no: NNX12AG21G), and US Geological Survey (USGS) Land Change Science Program.

Disclaimer. The USDA is an equal opportunity provider and employer. Any use of trade, firm, or product names is for descriptive purposes only and does not imply endorsement by the US Government. The findings and conclusions in this article are those of the author(s) and do not necessarily represent the views of the U.S. Fish and Wildlife Service.

References

Abler, D.G. and Shortle, J.S.: Climate change and agriculture in the Mid-Atlantic Region. Climate Res., 14 (3), 185-194, 2000.

Ainsworth, E.A. and Rogers, A.: The response of photosynthesis and stomatal conductance to rising [CO2]: mechanisms and environmental interactions. Plant Cell Environ., 30(3), 258-270, 2007.

Arnold, J.G., Moriasi, D.N., Gassman, P.W., Abbaspour, K.C., White, M.J., Srinivasan, R., Santhi, C., Harmel, R.D., Van Griensven, A., Van Liew, M.W. and Kannan, N.: SWAT: Model use, calibration, and validation. T. ASABE., 55(4), 1491-1508, 2012.

Brekke, L., Thrasher, B.L., Maurer, E.P. and Pruitt, T.: Downscaled CMIP3 and CMIP5 climate projections: release of downscaled CMIP5 climate projections, comparison with preceding information, and summary of user needs. US Department of the Interior, Bureau of Reclamation, Technical Service Center, Denver, Colorado, 2013.

Chaplot, V.: Water and soil resources response to rising levels of atmospheric CO 2 concentration and to changes in precipitation and air temperature. J. Hydrol. 337(1), 159-171, 2007.

Chesapeake Bay Program: http://www.chesapeakebay.net/discover/bay101/facts, last access: 31 May 2016

Chiang, S.L.: A runoff potential rating table for soils. J. Hydrol. 13, 54-62, 1971.

Denver, J.M., Tesoriero, A.J., and Barbaro, J.R.: Trends and Transformation of Nutrients and Pesticides in a Coastal Plain Aquifer System, United States. J. Environ. Qual. 39(1), 154-67, 2010.

Denver, J. M., Ator, S. W., Lang, M. W., Fisher, T. R., Gustafson, A. B., Fox, R., Clune, J. W., and McCarty, G. W.: Nitrate fate and transport through current and former depressional wetlands in an agricultural landscape, Choptank Watershed, Maryland, United States. J. Soil Water Conser. 69 (1), 1-16, 2014.

Eckhardt, K. and Ulbrich, U.: Potential impacts of climate change on groundwater recharge and streamflow in a central European low mountain range. J. Hydrol. 284(1), 244-252, 2003.

Ficklin, D.L., Luo, Y., Luedeling, E., and Zhang, M.: Climate change sensitivity assessment of a highly agricultural watershed using SWAT. J. Hydrol. 374 (1), 16-29, 2009.

Ficklin, D.L., Stewart, I.T., and Maurer, E.P.: Climate change impacts on streamflow and subbasin-scale hydrology in the upper Colorado River Basin. PLOS ONE, 8(8), e71297, 2013.

Field, C.B., Jackson, R.B., and Mooney, H.A.: Stomatal responses to increased CO2: implications from the plant to the global scale. Plant, Cell & Environment, 18(10), 1214-1225, 1995.

Fisher, T. R., Jordan, T. E., Staver, K. W., Gustafson, A. B., Koskelo, A. I., Fox, R. J., Sutton, A. J., Kana, T., Beckert, K. A., Stone, J. P., McCarty, G., and Lang, M.: The Choptank Basin in transition: intensifying agriculture, slow urbanization, and estuarine eutrophication, in: Coastal Lagoons: critical habitats of environmental change, edited by: Kennish, M. J. and Paerl, H. W., CRC Press, 135–165, 2010.

Gassman, P.W., Reyes, M.R., Green, C.H. and Arnold, J.G.: The soil and water assessment tool: historical development, applications, and future research directions. T. ASABE., 50(4), 1211-1250, 2007.

Gitau, M.W., and Chaubey, I.: Regionalization of SWAT Model Parameters for Use in Ungauged Watersheds. Water. 2(4), 849-71, 2010.

690 Glancey, J., Brown, B., Davis, M., Towle, L., Timmons, J., and Nelson, J.: Comparison of
691 Methods for Estimating Poultry Manure Nutrient Generation in the Chesapeake Bay
692 Watershed, available at: http://www.csgeast.org/2012annualmeeting/documents/
693 Glancey.pdf (last access: 25 September 2014), 2012.

694 Gombault, C., Madramootoo, C.A., Michaud, A., Beaudin, I., Sottile, M.F., Chikhaoui, M., and
695 Ngwa, F.: Impacts of climate change on nutrient losses from the Pike River watershed of
696 southern Québec. Can. J. of Soil Sci. 95(4), 337-358, 2015.

697 Hively, W.D., Hapeman, C.J., McConnell, L.L., Fisher, T.R., Rice, C.P., McCarty, G.W.,
698 Sadeghi, A.M., Whitall, D.R., Downey, P.M., de Guzmán, G.T.N. and Bialek-Kalinski,
699 K.: Relating nutrient and herbicide fate with landscape features and characteristics of 15
700 subwatersheds in the Choptank River watershed. Sci. Total Environ. 409(19), 3866-3878,
701 2011.

702 Howarth, R.W., Swaney, D.P., Boyer, E.W., Marino, R., Jaworski, N., and Goodale, C.: The
703 influence of climate on average nitrogen export from large watersheds in the
704 Northeastern United States. Biogeochemistry. 79(1-2), 163-186, 2006.

705 Jha, M., Arnold, J.G., Gassman, P.W., Giorgi, F. and Gu, R.R.: CLIMATE CHHANGE
706 SENSITIVITY ASSESSMENT ON UPPER MISSISSIPPI RIVER BASIN
707 STREAMFLOWS USING SWAT1. J. Am. Water Resour. As., 997-1015, 2006.

708 Jha, B. and Jha, M.K.: Rating Curve Estimation of Surface Water Quality Data Using
709 LOADEST. J Environ Prot. 4(8), 849-856, 2013.

710 Jordan, T.E., Correll, D.L. and Weller, D.E.: Relating nutrient discharges from watersheds to
711 land use and streamflow variability. Water Resour. Res. 33(11), 2579-2590, 1997.

712 Kiptala, J.K., Mul, M.L., Mohamed, Y.A. and Van der Zaag, P.: Modelling stream flow and
713 quantifying blue water using a modified STREAM model for a heterogeneous, highly
714 utilized and data-scarce river basin in Africa. Hydrol Earth Syst Sc. 18 (6), 2287-2303,
715 2014.

716 Lee, S., Yeo, I.Y., Sadeghi, A.M., McCarty, G.W. and Hively, W.D.: Prediction of climate
717 change impacts on agricultural watersheds and the performance of winter cover crops:
718 Case study of the upper region of the Choptank River Watershed, Proceedings of
719 the ASABE 1st Climate Change Symposium: Adaptation and Mitigation, Chicago, IL, 3-
720 5, May 2015

721 Lee, S., Yeo, I.-Y., Sadeghi, A. M., McCarty, W. M., Hively, W. D., and Lang, M. W.: Impacts
722 of Watershed Characteristics and Crop Rotations on Winter Cover Crop Nitrate Uptake
723 Capacity within Agricultural Watersheds in the Chesapeake Bay Region. PLOS ONE.
724 11(6), e0157637, 2016a.

725 Lee, C.J., Hirsch, R.M., Schwarz, G.E., Holtschlag, D.J., Preston, S.D., Crawford, C.G. and
726 Vecchia, A.V.: An evaluation of methods for estimating decadal stream loads. J
727 Hydrol. 542, 185-203, 2016b.

728 McCarty, G.W., McConnell, L.L., Hapeman, C.J., Sadeghi, A., Graff, C., Hively, W.D., Lang,
729 M.W., Fisher, T.R., Jordan, T., Rice, C.P., and Codling, E.E.: Water quality and
730 conservation practice effects in the Choptank River watershed. J. Soil Water
731 Conserv. 63(6), 461-474, 2008.

732 McCarty, G.W., Hapeman, C.J., Rice, C.P., Hively, W.D., McConnell, L.L., Sadeghi, A.M.,
733 Lang, M.W., Whitall, D.R., Bialek, K. and Downey, P.: Metolachlor metabolite (MESA)

reveals agricultural nitrate-N fate and transport in Choptank River watershed. Sci. Total Environ. 473, 473-482, 2014.

Mearns, L.O., Hulme, M., Carter, T.R., Leemans, R., Lal, M., Whetton, P., Hay, L., Jones, R.N., Kittel, T., Smith, J. and Wilby, R.: Climate scenario development, 2001.

Meinshausen, M., Smith, S.J., Calvin, K., Daniel, J.S., Kainuma, M.L.T., Lamarque, J.F., Matsumoto, K., Montzka, S.A., Raper, S.C.B., Riahi, K. and Thomson, A.G.: The RCP greenhouse gas concentrations and their extensions from 1765 to 2300. Clim. Chang. 109(1-2), 213, 2011.

Moriasi, D. N., Arnold, J. G., Van Liew, M. W., Bingner, R. L., Harmel, R. D., and Veith, T. L.: Model evaluation guidelines for systematic quantification of accuracy in watershed simulations. T. ASABE. 50(3), 885-900, 2007.

Najjar, R., Patterson, L., and Graham, S.: Climate simulations of major estuarine watersheds in the Mid-Atlantic region of the US. Climatic Change, 95 (1-2), 139-168, 2009.

Najjar, R.G., Pyke, C.R., Adams, M.B., Breitburg, D., Hershner, C., Kemp, M., Howarth, R., Mulholland, M.R., Paolisso, M., Secor, D. and Sellner, K.: Potential climate-change impacts on the Chesapeake Bay. Estuar. Coast. Shelf S. 86(1), 1-20, 2010.

Neitsch, S. L., Arnold, J. G., Kiniry, J. R., and Williams, J. R.: Soil and Water Assessment Tool. Theoretical Documentation; Version 2009, Texas Water Resources Institute Technical Report No. 406, Texas A&M University System, College Station, TX, 2011.

753 Parry, M.L., Rosenzweig, C., Iglesias, A., Livermore, M. and Fischer, G.: Effects of climate
754 change on global food production under SRES emissions and socio-economic
755 scenarios. Global Environ. Chang. 14(1), 53-67, 2004.

756 Pervez, M.S. and Henebry, G.M.: Assessing the impacts of climate and land use and land cover
757 change on the freshwater availability in the Brahmaputra River basin. J Hydrol: Regional
758 Studies, 3, 285-311, 2015.

759 Praskievicz, S.: IMPACTS OF PROJECTED CLIMATE CHANGES ON STREAMFLOW
760 AND SEDIMENT TRANSPORT FOR THREE SNOWMELT-DOMINATED RIVERS
761 IN THE INTERIOR PACIFIC NORTHWEST. River Res. Appl. 2014.

762 Qiu, L., Zheng, F., and Yin, R.: SWAT-based runoff and sediment simulation in a small
763 watershed, the loessial hilly-gullied region of China: capabilities and challenges. Int. J.
764 Sediment Res. 27(2): 226-234, 2012.

765 Rogers, C.E. and McCarty, J.P.: Climate change and ecosystems of the Mid-Atlantic
766 Region. Climate Res. 14(3), 235-244, 2000.

767 Runkel, R.L., Crawford, C.G. and Cohn, T.A., 2004. Load Estimator (LOADEST): A
768 FORTRAN program for estimating constituent loads in streams and rivers. U.S.
769 Geological Survey Paper, Reston, Virginia, 2004

770 Sexton, A.M., Sadeghi, A.M., Zhang, X., Srinivasan, R. and Shirmohammadi, A.: Using
771 NEXRAD and rain gauge precipitation data for hydrologic calibration of SWAT in a
772 northeastern watershed. T. ASABE, 53(5), 1501-1510, 2010.

773 Seo, M., Yen, H., Kim, M.K. and Jeong, J.: Transferability of SWAT Models between
774 SWAT2009 and SWAT2012. J. Environ Qual, 43(3), 869-880, 2014.

775 Sharifi, A., Lang, M.W., McCarty, G.W., Sadeghi, A.M., Lee, S., Yen, H., Rabenhorst, M.C.,
776 Jeong, J. and Yeo, I.Y.: Improving Model Prediction Reliability through Enhanced
777 Representation of Wetland Soil Processes and Constrained Model Auto Calibration–A
778 Paired Watershed Study. J. Hydrol, 541, 1088-1103, 2016.

779 Shrestha, R.R., Dibike, Y.B. and Prowse, T.D.: Modelling of climate-induced hydrologic
780 changes in the Lake Winnipeg watershed. J. Great Lakes Res. 38, 83-94, 2012.

781 Singh, A., Imtiyaz, M., Isaac, R.K. and Denis, D.M.: Assessing the performance and uncertainty
782 analysis of the SWAT and RBNN models for simulation of sediment yield in the Nagwa
783 watershed, India. Hydrolog. Sci. J. 59(2), 351-364, 2014.

784 Suddick, E.C., Whitney, P., Townsend, A.R. and Davidson, E.A.: The role of nitrogen in climate
785 change and the impacts of nitrogen–climate interactions in the United States: foreword to
786 thematic issue. Biogeochemistry. 114(1-3), 1-10, 2013.

787 Tiner, R. W., Burke, D. G.: Wetlands of Maryland. US Fish and Wildlife Service, Hadly,
788 Massachusetts, 261 pp, 1995.

789 Uniyal, B., Jha, M.K. and Verma, A.K.: Assessing climate change impact on water balance
790 components of a river basin using SWAT model. Water Resour. Manag. 29(13), 4767-
791 4785, 2015.

792 Van Liew, M.W., Feng, S. and Pathak, T.B.: Climate change impacts on streamflow, water
793 quality, and best management practices for the shell and logan creek watersheds in
794 Nebraska, USA. Int. J. Agric. Biol. Eng. 5(1), 13-34, 2012.

795 Wang, R., Kalin, L., Kuang, W. and Tian, H.: Individual and combined effects of land use/cover
796 and climate change on Wolf Bay watershed streamflow in southern Alabama. Hydrol.
797 Process. 28(22), 5530-5546, 2014.

798 Woznicki, S.A., Nejadhashemi, A.P. and Parsinejad, M.: Climate change and irrigation demand:
799 Uncertainty and adaptation. J. Hydrol.: Regional Studies. 3, 247-264, 2015.

800 Wu, Y., Liu, S. and Gallant, A.L.: Predicting impacts of increased CO 2 and climate change on
801 the water cycle and water quality in the semiarid James River Basin of the Midwestern
802 USA. Sci. Total Environ. 430, 150-160, 2012a.

803 Wu, Y., Liu, S. and Abdul-Aziz, O.I.: Hydrological effects of the increased CO2 and climate
804 change in the Upper Mississippi River Basin using a modified SWAT. Climatic
805 Change, 110(3-4), 977-1003, 2012b.

806 Yang, Q. and Zhang, X.: Improving SWAT for simulating water and carbon fluxes of forest
807 ecosystems. Sci. Total Environ. 569, 1478-1488, 2016.

808 Yeo, I.Y., Lee, S., Sadeghi, A.M., Beeson, P.C., Hively, W.D., McCarty, G.W. and Lang, M.W.:
809 Assessing winter cover crop nutrient uptake efficiency using a water quality simulation
810 model. Hydrol. Earth Syst. Sc. 18(12), 5239-5253, 2014.

811 Zhang, H., Yuan, W., Dong, W. and Liu, S.: Seasonal patterns of litterfall in forest ecosystem
812 worldwide. Ecol Complex. 20, 240-247, 2014.

List of Tables

Table 3. List of calibrated parameters

Table 4. Climate sensitivity scenarios developed by modifying baseline values

Table 5. Model performance measures for monthly stream flow and nitrate loads

Table 6. Seasonal ET (mm/ha/10^2) under climate sensitivity scenarios

Table 7. 14-year average of hydrologic variables under the baseline and GCM scenarios

Table 1. Soil properties and land use distribution of the Tuckahoe Creek Watershed (TCW) and Greensboro Watershed (GW) (adapted from Lee et al. (2016a))

Land use	TCW	GW
Agriculture	54.0 % [69.5% / 30.5 %]	36.1 % [32.8% / 67.2 %]
Forest	32.8 %	48.3 %
Pasture	8.4 %	9.3 %
Urban	4.2 %	5.6 %
Water body	0.6 %	0.7 %
Hydrologic soil groups (HSGs)	TCW	GW
A	0.3 %	3.1 %

B	55.8 %	22.4 %
C	2.2 %	4.2 %
D	41.7 %	70.3 %

Note: Values in parenthesis [], denote the proportion of well-drained soils (HSG-A&B) and poorly-drained soils (HSG-C&D) used for agricultural lands, respectively.

Table 2. List of the SWAT model input data

Data	Source	Description	Year
DEM	MD-DNR	LiDAR-based 2 meter resolution	2006
Land use	USDA-NASS	Cropland Data Layer (CDL)	2008 - 2012
	MRLC	National Land Cover Database (NLCD)	2006
	USDA-FSA-APFO	National Agricultural Imagery Program digital Orthophoto quad imagery	1998
	US Census Bureau	TIGER road map	2010
Soils	USDA-NRCS	Soil Survey Geographical Database (SSURGO)	2012
Climate	NCDC	Daily precipitation and temperature	1999 - 2014
Stream flow	USGS	Monthly stream flow	2001 - 2014
Water quality	USGS and CBP	Daily grab nitrate samples	2001 - 2014

Note: MD-DNR: Maryland Department of Natural Resources, USDA-NASS: USDA-National Agricultural Statistics Service, MRLC: Multi-Resolution Land Characteristics Consortium, USDA-FSA-APFO: USDA-Farm Service Agency-Aerial Photography Field Office, TIGER: Topologically Integrated Geographic Encoding and Referencing, and USDA-NRCS: USDA-Natural Resources Conservation Service.

Table 3. List of calibrated parameters

Parameter	Variable	Description (unit)	Range	Calibrated value	
				TCW	GW
CN2#	Stream flow	Curve number	-50 - 50 %	-30 %	0%
ESCO#		Soil evaporation compensation factor	0 - 1	1	0.95
SURLAG#		Surface runoff lag coefficient	0.5 - 24	0.5	0.5
SOL_AWC#		Available water capacity of the soil layer (mm H2O mm soil^{-1})	-50 - 50 %	- 10%	- 1%
SOL_K#		Saturated hydraulic conductivity (mm hr^{-1})	-50 - 50 %	50 %	49 %

SOL_Z[#]		Depth from soil surface to bottom of layer (mm)	-50 - 50 %	-20 %	-31 %
ALPHA_BF[#]		Base flow recession constant (1 $days^{-1}$)	0 - 1	0.07	0.051
GW_DELAY[#]		Groundwater delay time (days)	0 - 500	120	45
GW_REVAP[#]		Groundwater "revap" coefficient	0.02 - 0.2	0.10	0.02
RCHRG_DP[#]		Deep aquifer percolation fraction	0 - 1	0.01	0.05
GWQMN[#]		Threshold depth of water in the shallow aquifer required for return flow to occur (mm)	0 - 5000	1.9	1.0
CH_K2[#]		Effective hydraulic conductivity (mm hr^{-1})	0 - 150	0	20
CH_N2[#]		Manning coefficient	0.01 - 0.3	0.29	0.021
NPERCO[†]	Nitrate	Nitrogen percolation coefficient	0.01 - 1	0.5	0.2
N_UPDIS[†]		Nitrogen uptake distribution parameter	5 - 50	50	50
ANION_EXCL[†]		Fraction of porosity from which anions are excluded	0.1 - 0.7	0.59	0.6
ERORGN[†]		Organic N enrichment ratio for loading with sediment	0 - 5	4.92	4.1
BIOMIX[†]		Biological mixing efficiency	0.01 - 1	0.01	0.01
SOL_NO3[§]		Initial NO3 concentration in soil layer (mg N kg^{-1})	0 - 100	11.23	0
CDN[$]		Denitrification exponential rate coefficient	0 - 3.0	0.3	1.8
SDNCO[$]		Denitrification threshold water content	0.1 - 1.1	1.0	1.0

* refers to a default value. The ranges of parameters with superscripts (#, †, §, $) were adapted from Gitau and Chaubey (2010), Yeo et al. (2014), Seo et al. (2012), Neitsch et al. (2011), respectively.

Table 4. Climate sensitivity scenarios developed by modifying baseline values

Scenario	Percent increase of precipitation (%)	Absolute increase of temperature (°C)	Replacement of CO_2 (ppm)
Baseline	0	0	330
1	0	0	590
2	0	0	850
3	11	0	330
4	21	0	330
5	0	2.9	330
6	0	5.0	330

Table 5. Model performance measures for monthly stream flow and nitrate loads

Period	Variable	Stream flow		Nitrate loads	
		TCW	GW	TCW	GW
Calibration	NSE	0.723** (0.828***)	0.686** (0.719**)	0.623*	0.702**
	RSR	0.523**	0.556**	0.610*	0.542**
	P-bias (%)	-5.8***	-3.2***	-9.8***	-4.1***
Validation	NSE	0.674** (0.556*)	0.790*** (0.727**)	0.604*	0.567*
	RSR	0.566**	0.454***	0.624*	0.652*
	P-bias (%)	17.8**	13***	-5.6***	-12.1***

Model performances were rated based on the criteria of Moriasi et al. (2007); * Satisfactory, ** Good, and *** Very Good; Satisfactory ($0.5 < NSE \leq 0.65$, $0.6 < RSR \leq 0.7$, and $\pm 15 \leq$ P-bias $<$

± 25), ** Good (0.65 < NSE ≤ 0.75, 0.5 < RSR ≤ 0.6, and ± 10 ≤ P-bias < ± 15), and *** Very Good (0.75 < NSE ≤ 1.0, 0.0 < RSR ≤ 0.5, P-bias < ± 10). A value in parentheses indicates NSE for the natural logarithm of stream flow.

Table 6. 14-year average of hydrologic variables under the baseline and GCM scenarios

Variables	TCW			GW		
	Baseline	GCM scenario	Relative change (%)	Baseline	GCM scenario	Relative change (%)
Stream flow (m^3 s^{-1} ha^{-1} 10^4)	1.5	2.5 (2.3 – 2.8)	70	1.7	2.5 (2.3 – 2.8)	50
ET (mm ha^{-1})	2.7	1.8	-32	2.3	1.7	-26
Nitrate loads (kg N ha^{-1})	12.5	20.8 (19.8 – 22.0)	66	5.3	8.2 (7.8 – 8.9)	56

Note: The numbers within parenthesis indicates the maximum and minimum values of simulations with five GCM data. Relative change indicates the percent changes in the ensemble mean relative to the baseline value.

List of Figures

Figure 5. The responses of crop biomass growth to the climate sensitivity scenario: (a & b & c) corn and (d & e & f) soybean.

Figure 6. 14-year average of seasonal hydrologic variables under the baseline and climate sensitivity scenarios at the watershed scale: (a) water and (b) nitrate yields.

Figure 7. Monthly average of (a) mean temperature and (b) cumulative precipitation for the baseline (2001 – 2014) and future (2083 – 2098) periods.

Figure 8. 14-year average of monthly water and nitrate yields under the baseline and GCM scenarios. The descriptions of abbreviation are illustrated in the caption of Figure 6.

Figure 9. Crop biomass growth under the baseline and GCM scenarios: (a) corn and (b) soybean.

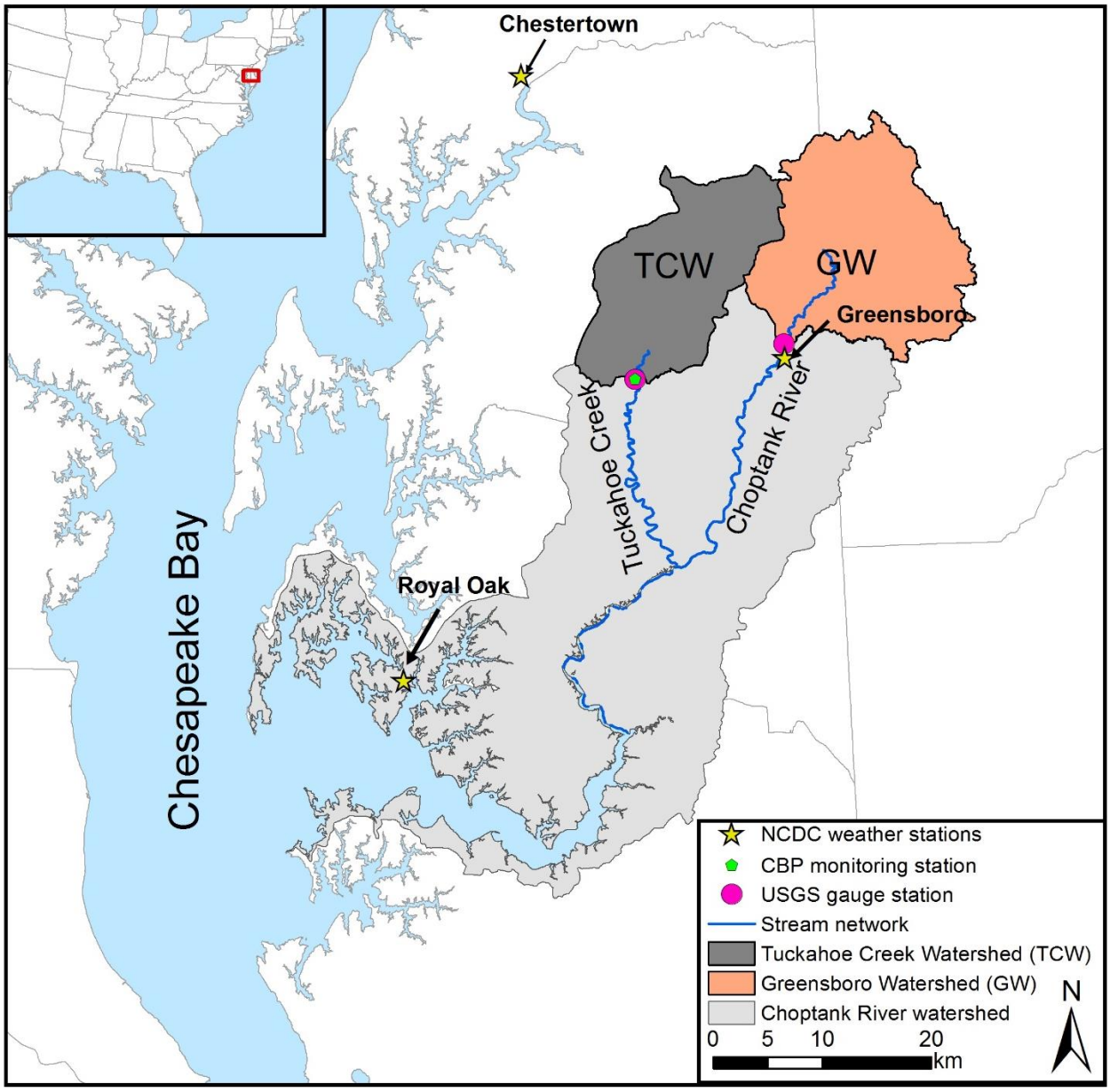

952

953 **Figure 1.** The location of the Tuckahoe Creek Watershed (left) and Greensboro Watershed (right)
954 (adapted from Lee et al. (2016a))

955

956

957

958

959

960

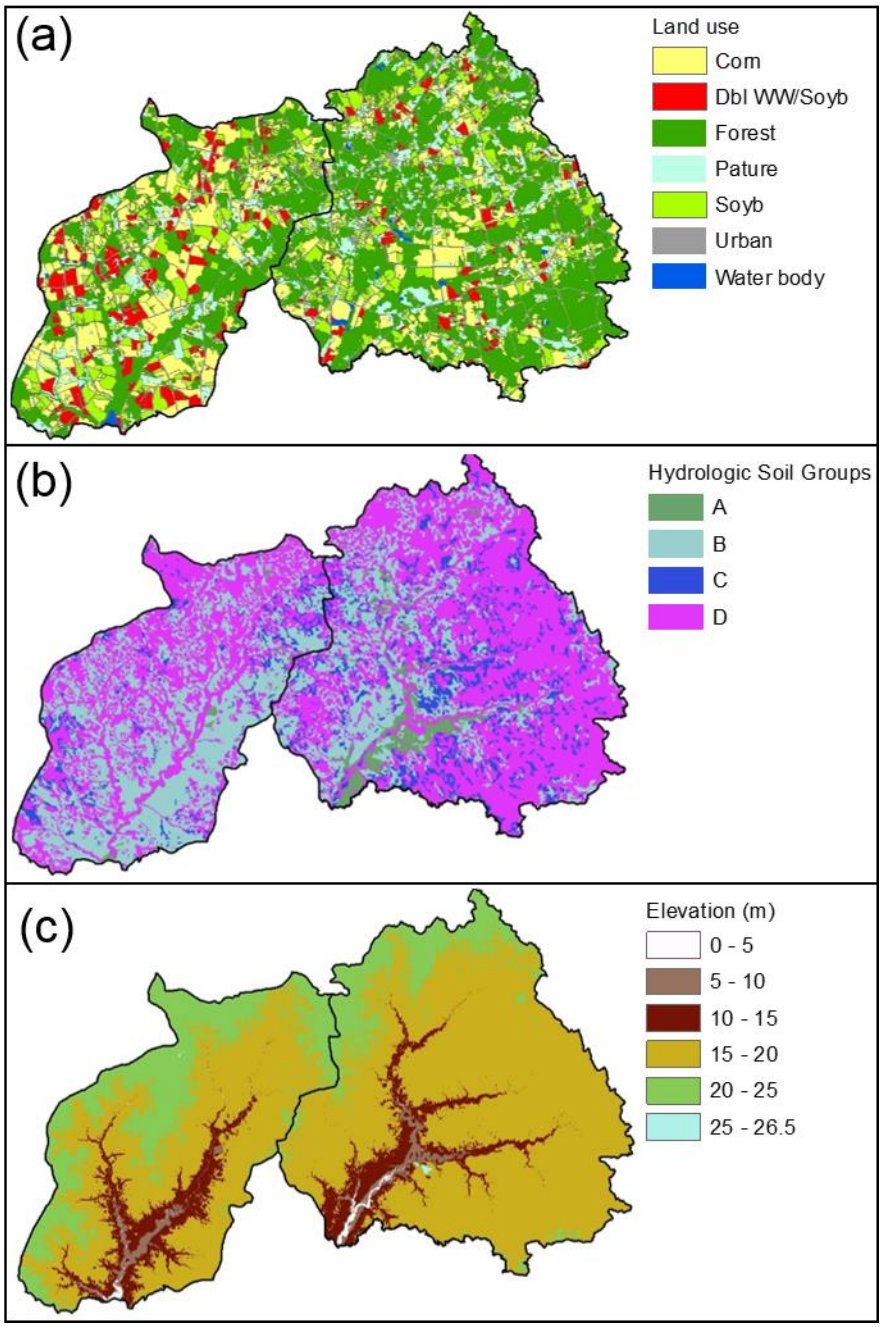

961

962 **Figure 2.** The physical characteristics of the Tuckahoe Creek Watershed (left) and Greensboro
963 Watershed (right); (a) land use, (b) hydrologic soil groups, and (c) elevation (adapted from Lee
964 et al. (2016a)).

965 Note: Dbl WW/Soyb stands for double crops of winter wheat and soybean in a year. Hydrologic
966 soil groups (HSGs) are characterized as follows: Type A- well-drained soils with 7.6-11.4 mm
967 hr^{-1} water infiltration rate; Type B - moderately well-drained soils with 3.8-7.6 mm hr^{-1}; Type C -
968 moderately poorly-drained soils with 1.3-3.8 mm hr^{-1}; Type D – poorly-drained soils with 0-1.3
969 mm hr^{-1} (Netisch et al., 2011).

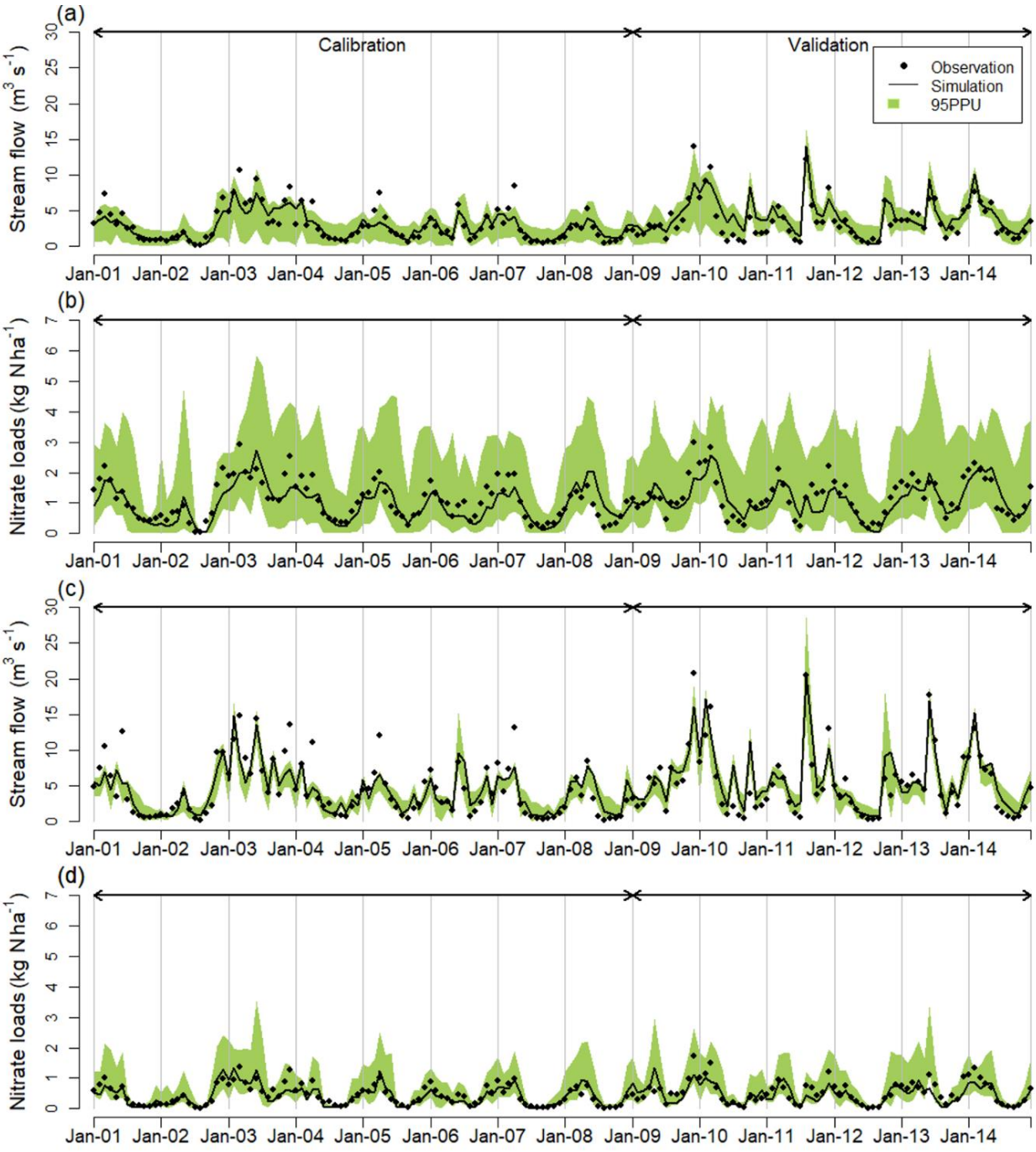

970

971 **Figure 3**. Simulated and observed monthly stream flow and nitrate loads for the (a & b) TCW
972 and (c & d) GW during calibration and validation periods.

973 Note: 95 PPU stands for 95 percent prediction uncertainty.

974

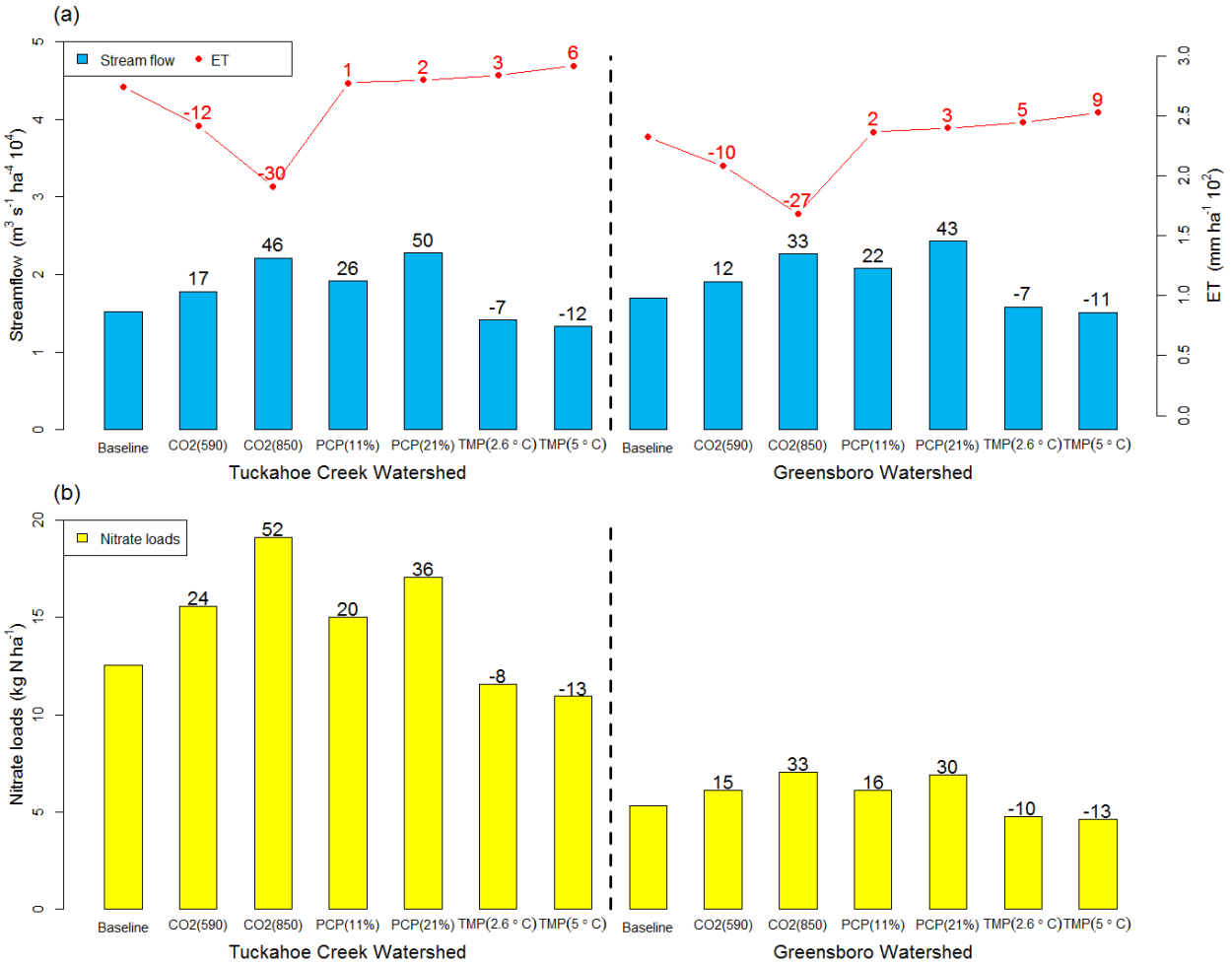

975

976 **Figure 4**. 14-year average of annual hydrologic variables under the baseline and climate
977 sensitivity scenarios at the watershed scale: (a) stream flow and evapotranspiration (ET), and (b)
978 nitrate loads.

979 Note: The red and black numerical values above the bar and the dot graphs, respectively, indicate
980 the relative changes (%) in hydrologic variables for climate sensitivity scenarios relative to the
981 baseline scenario [relative change (%) = (Sensitivity Scenarios – Baseline) / Baseline × 100].
982 PCP and TMP stand for precipitation and temperature, respectively.

983

984

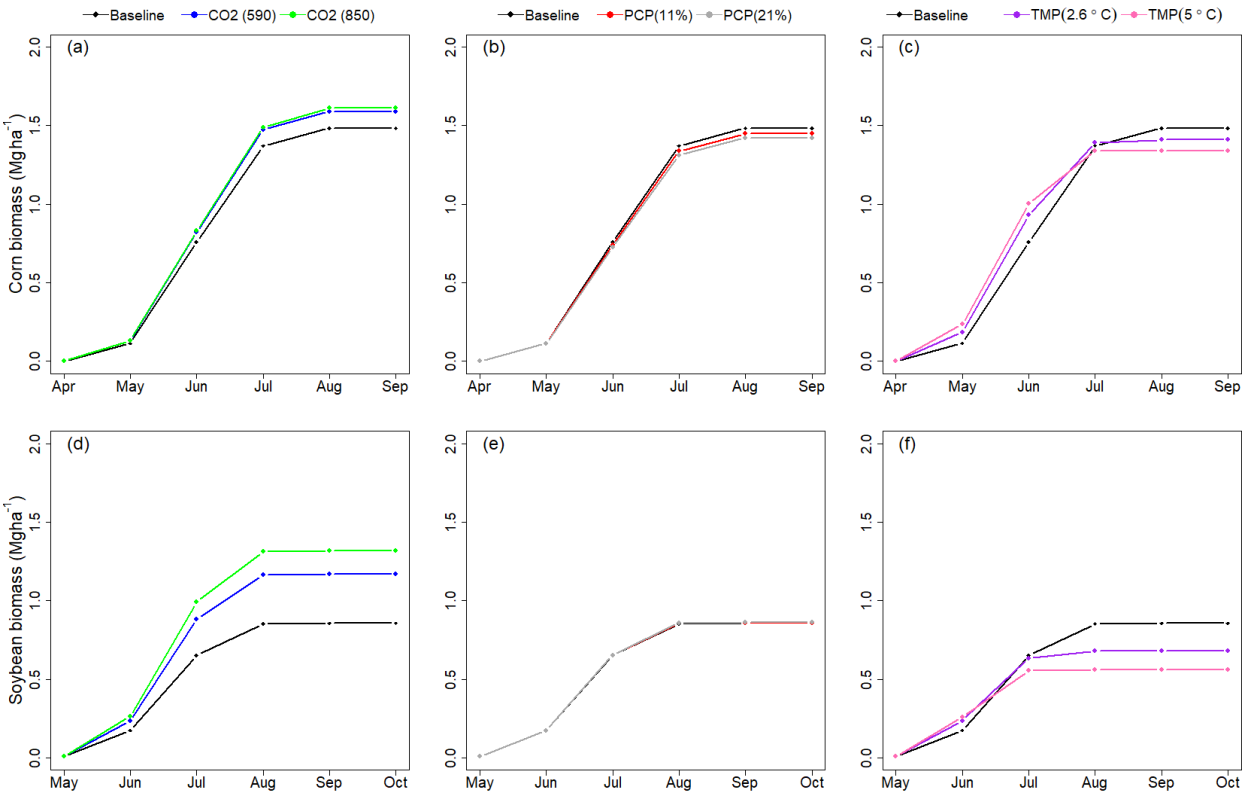

985

986 **Figure 5.** The responses of crop biomass growth to the climate sensitivity scenario: (a & b & c)
987 corn and (d & e & f) soybean.

988 Note: PCP and TMP in the legend stand for precipitation and temperature, respectively.

989

990

991

992

993

994

995

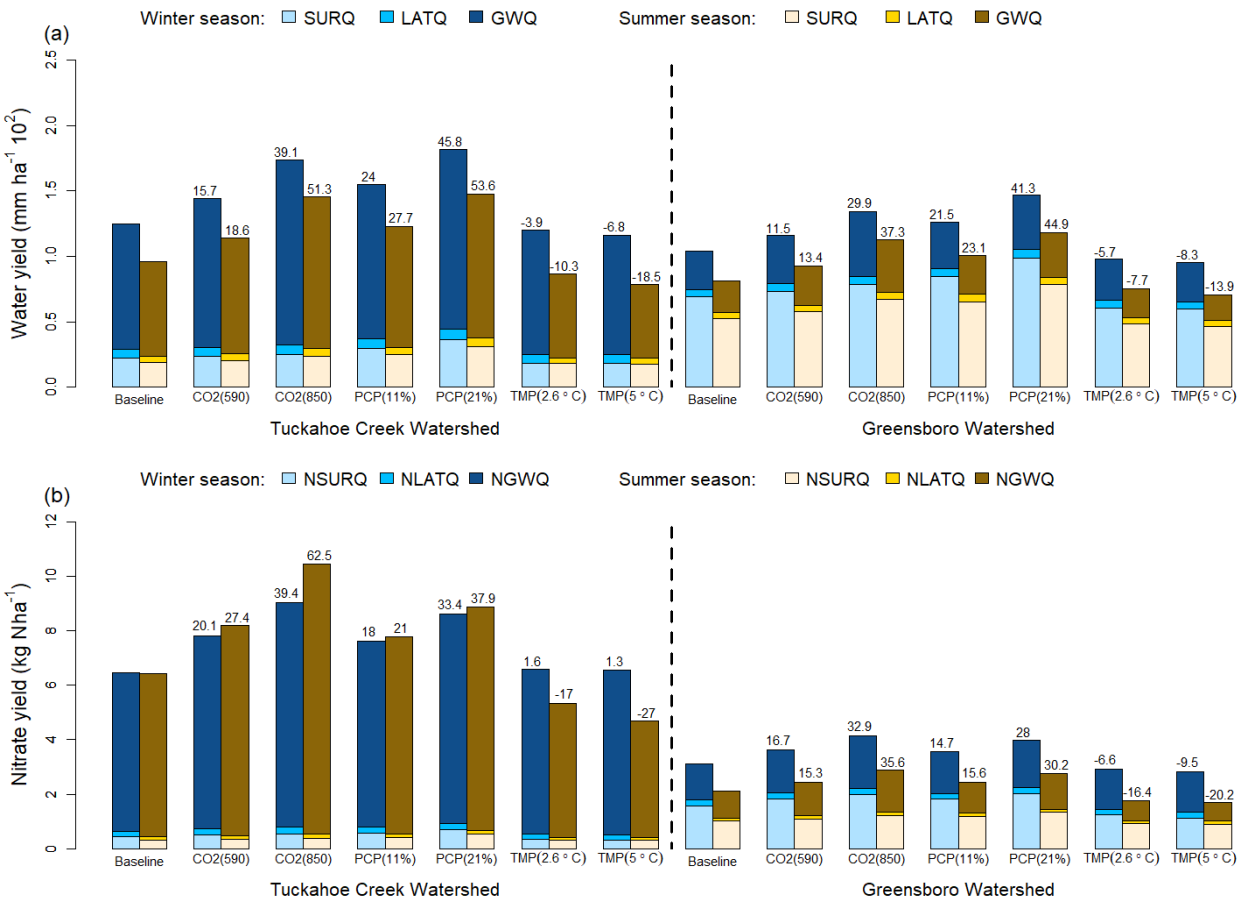

Figure 6. 14-year average of seasonal hydrologic variables under the baseline and climate sensitivity scenarios at the watershed scale: (a) water and (b) nitrate yields.

Note: The number on the bar graph indicates the relative changes (%) in hydrologic variables for climate sensitivity scenarios relative to the baseline scenario. Water and nitrate yields indicate the summations of water and nitrate fluxes transported from lands to streams by surface runoff, lateral flow, and groundwater flow. PCP and TMP stand for precipitation and temperature, respectively. SURQ, LATQ, and GWQ indicate water fluxes transported by surface runoff, lateral flow, and groundwater flow, respectively. NSURQ, NLATQ, and NGWQ indicate nitrate fluxes transported by surface runoff, lateral flow, and groundwater flow, respectively.

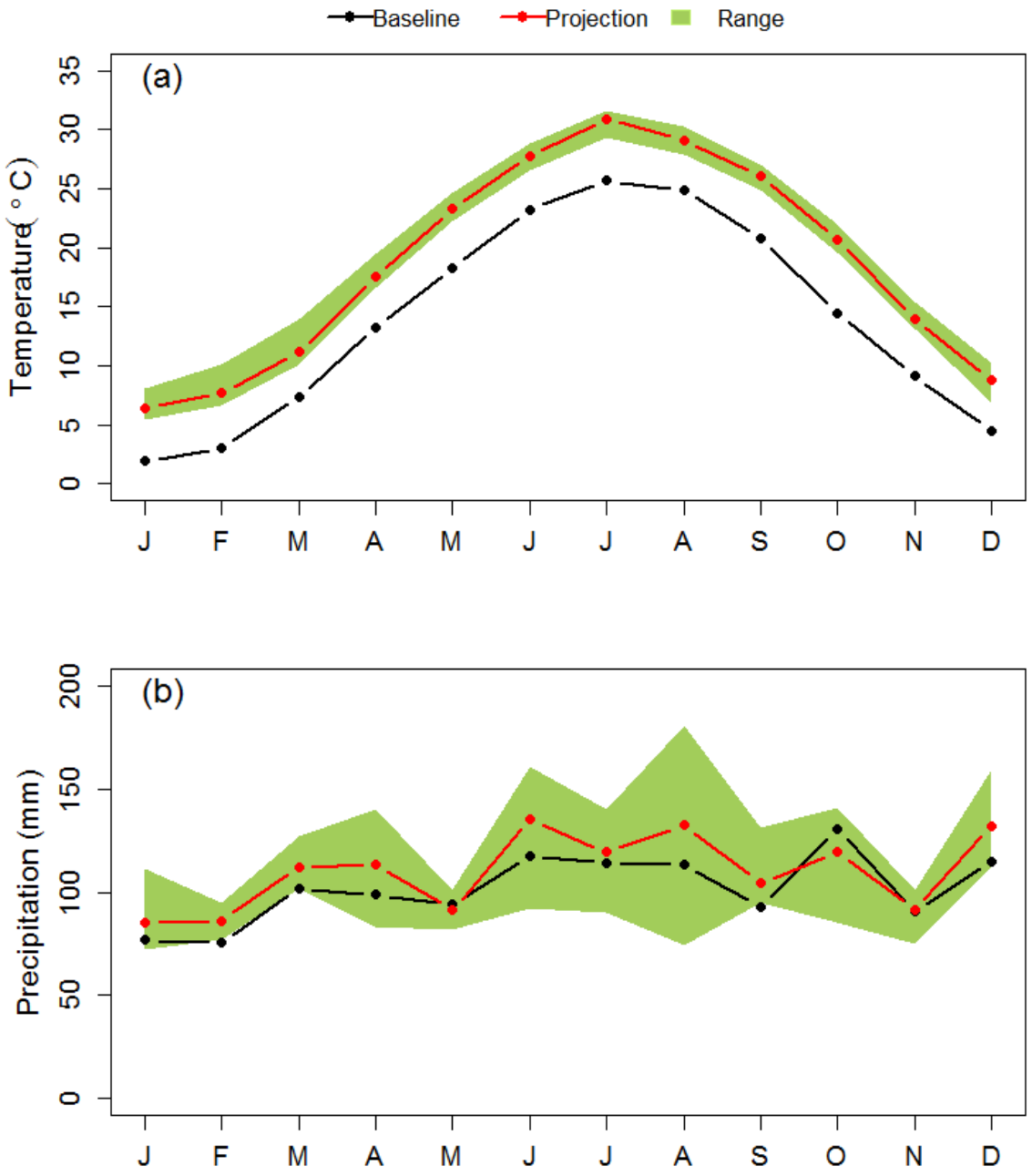

1010

1011 **Figure 7.** Monthly average of (a) mean temperature and (b) cumulative precipitation for the
1012 baseline (2001 – 2014) and future (2085 – 2098) periods.

1013 Note: Projection stands for the ensemble mean of five GCM data, and the range stands for the
1014 interval between the maximum and minimum values of five GCM data.

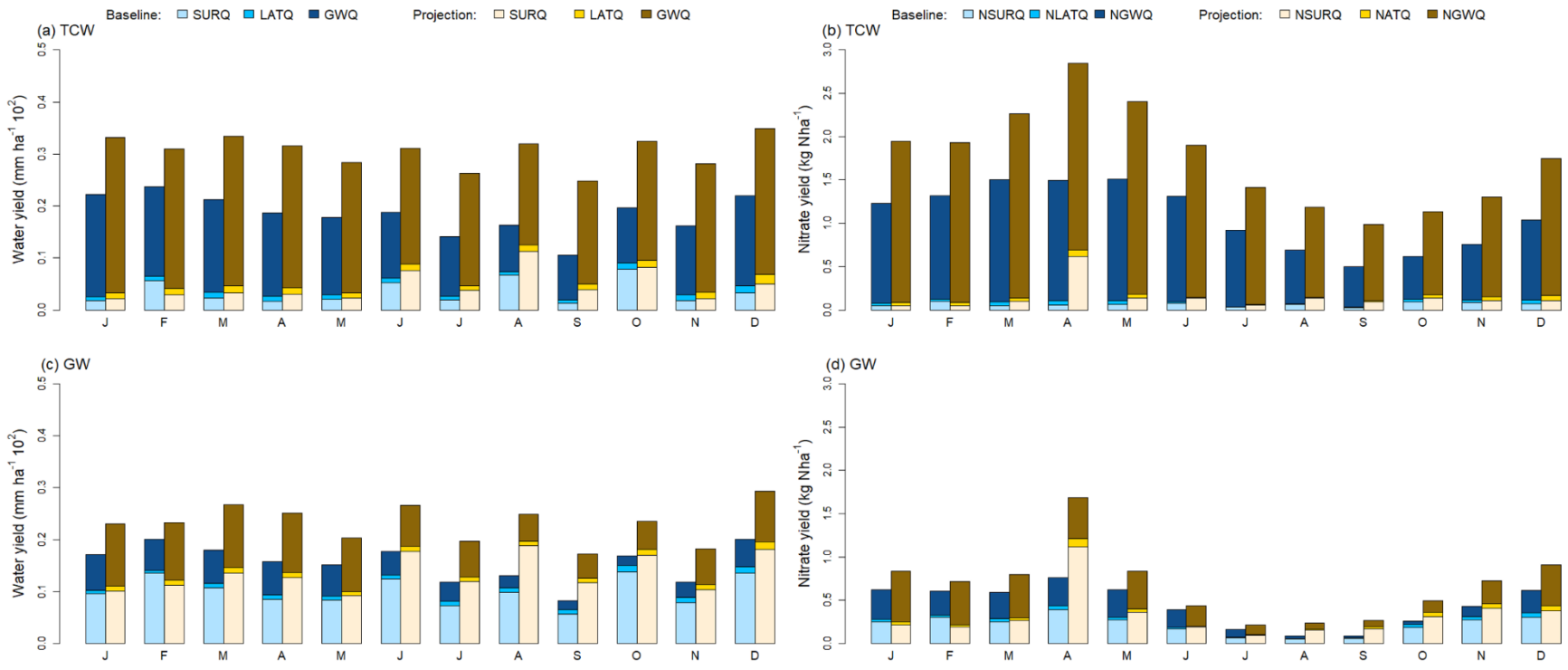

Figure 8. 14-year average of monthly water and nitrate yields under the baseline and GCM scenarios.

Note: The descriptions of abbreviation are available in the caption of Figure 6.

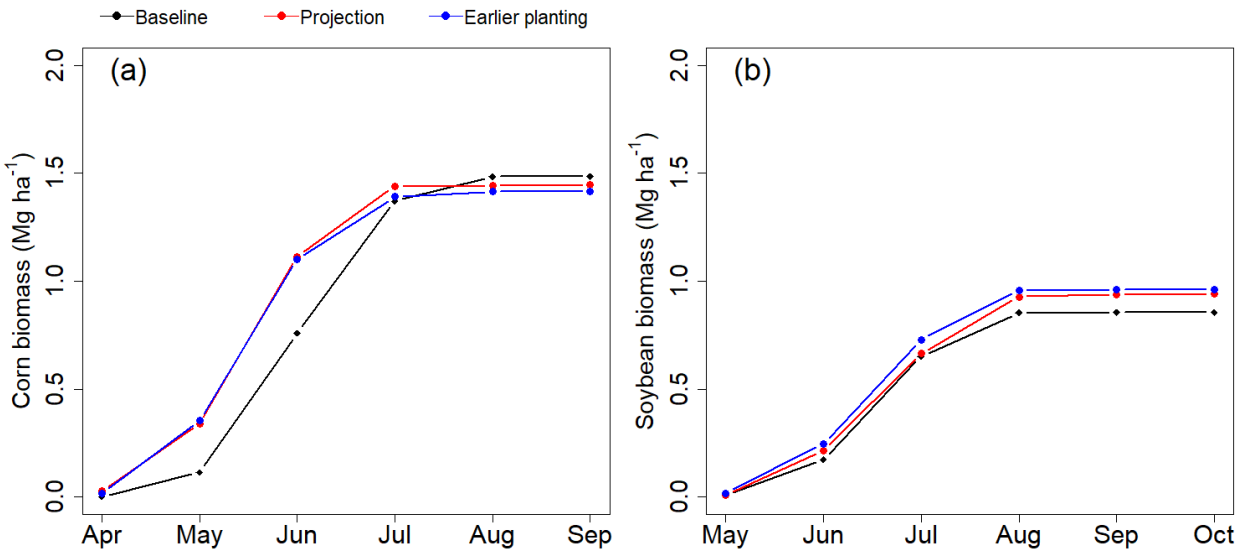

Figure 9. Crop biomass growth under the baseline and GCM scenarios: (a) corn and (b) soybean.

Note: Projection stands for the simulated biomass plantd on the original planting dates under the GCM scenario. Earlier planting indicates the simulated biomass planted 10 days earlier than the original planting dates under the GCM scenario.

List of Appendices

Table A1. Management schedules for the baseline scenario (adapted from Lee et al. (2016a))

Baseline scenario (no winter cover crop)			
Crop	Planting	Fertilizer	Harvest
Corn (after corn)	Apr. 30 (no-till)	157 kg N ha^{-1} of poultry manure on Apr. 20 45 kg N ha^{-1} of sidedress 30% UAN on Jun. 7	Oct. 3
Corn (after Soybean and Double crop soybean)	Apr. 30 (no-till)	124 kg N ha^{-1} of poultry manure on Apr. 20 34 kg N ha^{-1} of sidedress 30% UAN on Jun. 7	Oct. 3
Soybean	May 20 (no-till)		Oct. 15
Double crop winter wheat (Dbl WW)	Oct. 10	34 kg N ha^{-1} of sidedress 30% UAN on Oct. 8 45 kg N ha^{-1} of sidedress 30% UAN on Mar. 1 67 kg N ha^{-1} of sidedress 30% UAN on Apr. 5	Jun. 27
Double crop soybean (Dbl Soyb)	Jun. 29		Nov. 1

Note: UAN stands for Urea-Ammonium Nitrate. The typical nitrogen content for poultry manure is assumed as 2.8% (Glancey et al., 2012).

Table A2. Five GCMs used to the GCM scenario

Num.	Model	Full name	Modeling Group
1	BCC-CSM1-1.1	Beijing Climate Center (BCC) - Climate System Model (CSM)	Beijing Climate Center, China Meteorological Administration
2	CCSM4.1	Community Climate System Model (CCSM) 4.1	National Center for Atmospheric Research
3	GFDL-ESM2G.1	Geophysical Fluid Dynamics Laboratory (GFDL) - Earth System Model (ESM)	NOAA Geophysical Fluid Dynamics Laboratory
4	IPSL-CM5A-LR.1	Institut Pierre-Simon Laplace (IPSL) - Climate Model(CM)5A-Low Resolution	Institut Pierre-Simon Laplace
5	MIROC-ESM-CHEM.1	An atmospheric chemistry coupled version of Model for Interdisciplinary Research on Climate (MIROC) - Earth System Model (ESM)	Japan Agency for Marine-Earth Science and Technology, Atmosphere and Ocean Research Institute (The University of Tokyo), and National Institute for Environmental Studies

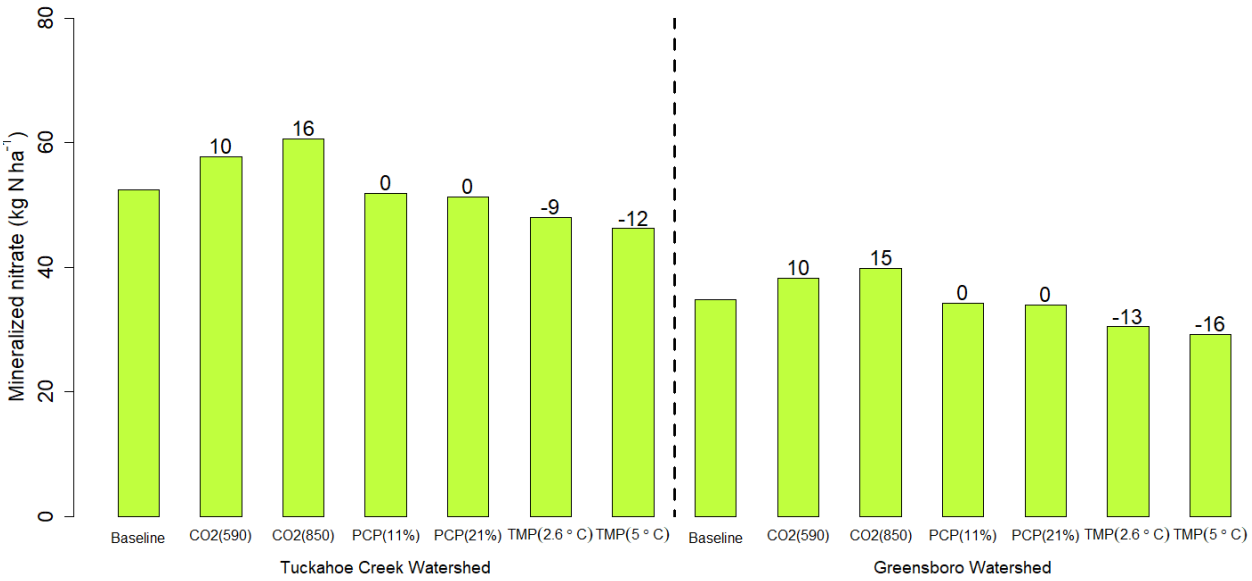

Figure A3. 14-year average of annual mineralized nitrate during winter seasons (Oct. – Mar.) under the baseline and climate sensitivity scenarios at the watershed scale.

Note: The black numerical values above the bar graph indicate the relative changes (%) in hydrologic variables for climate sensitivity scenarios relative to the baseline scenario [relative change (%) = (Sensitivity Scenarios – Baseline) / Baseline × 100]. PCP and TMP stand for precipitation and temperature, respectively.

Table A4. Seasonal ET (mm ha^{-1} 10^2) under climate sensitivity scenarios

Scenario	Corn		Soybean	
	Winter	Summer	Winter	Summer
Baseline	0.74	2.00	0.68	1.64
CO_2 (590 ppm)	0.65	1.77	0.59	1.49
CO_2 (850 ppm)	0.50	1.40	0.46	1.22
PCP (11 %)	0.75	2.03	0.68	1.68
PCP (21 %)	0.75	2.05	0.69	1.71
TMP (2.6 °C)	0.81	2.03	0.77	1.67
TMP (5.0 °C)	0.87	2.05	0.83	1.70

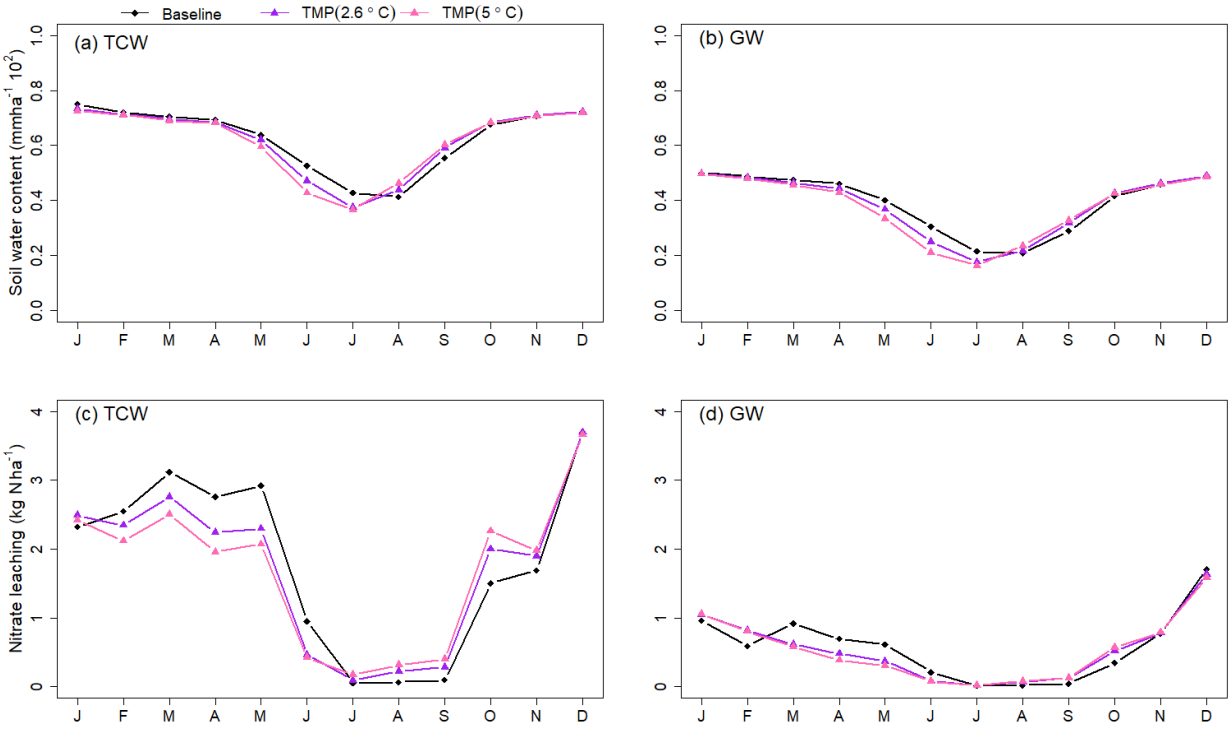

Figure A5. Changes in (a & b) soil water content and (c & d) nitrate leaching under temperature increase

Note: TMP stands for temperature, respectively.